

HCMV MANIPULATION OF HOST CHOLESTERYL ESTER METABOLISM

by

Elizabeth Dahlmann

---

Copyright © Elizabeth Dahlmann 2019

A Thesis Submitted to the Faculty of the

DEPARTMENT OF IMMUNOBIOLOGY

In Partial Fulfillment of the Requirements

For the Degree of

MASTER OF SCIENCE  
WITH A MAJOR IN MOLECULAR MEDICINE

In the Graduate College

THE UNIVERSITY OF ARIZONA

2019

THE UNIVERSITY OF ARIZONA  
GRADUATE COLLEGE

As members of the Master's Committee, we certify that we have read the thesis prepared by **Elizabeth Dahmann**, titled **HCMV Manipulation of Host Cholesteryl Ester Metabolism** and recommend that it be accepted as fulfilling the thesis requirement for the Master's Degree.



**Dr. Felicia Goodrum**

Date: 12/19/18



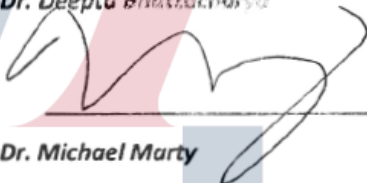
**Dr. John Purdy**

Date: 12/17/2018



**Dr. Deepta Bhattacharya**

Date: 12/19/18



**Dr. Michael Marty**

Date: 12/19/2019

Final approval and acceptance of this thesis is contingent upon the candidate's submission of the final copies of the thesis to the Graduate College.

I hereby certify that I have read this thesis prepared under my direction and recommend that it be accepted as fulfilling the Master's requirement.



**Felicia Goodrum**

Date: 12/19/18

**Associate Professor**

**Department of Immunobiology**

## Acknowledgements

I would like to thank Yuecheng Xi for developing and testing the PERK CRISPR knockout cells, as well as performing western blot confirmation on the AD<sub>sub</sub>UL37x1 virus. I am grateful for Lisa Wise, who assisted with establishing methods in the lab and assisted in LC-MS/MS development. I am thankful for my graduate committee, who have supported my education and provided me with valuable advice. I would also like to thank John Purdy for his advice and guidance as my advisor. Further, I would like to thank John Purdy for running LC-MS/MS lipids from cells infected with the AD<sub>sub</sub>UL37x1 virus.

Finally, I would like to thank my friends and family. Thank you for supporting me throughout this process, whether it be through words or actions. In particular, I would like to thank my dog Lexa. I'm sorry I didn't get to take you on as many walks as you would have liked. I promise to change that once I'm done with grad school.

## Table of Contents

List of Figures and Tables .....	6
Abstract .....	8
Chapter 1: Literature Review .....	9
1.1 Human Cytomegalovirus.....	9
Epidemiology and Health Implications .....	9
Human Cytomegalovirus Biology.....	15
Manipulation of Cellular Metabolism .....	16
1.2. Cholesteryl Esters.....	20
Structure and function .....	21
Cellular acquisition of CE .....	22
Sterol O-Acyltransferases 1-2.....	23
Roles of SOAT in metabolic diseases.....	25
Manipulation of CE by viruses .....	27
Chapter 2: Materials and Methods .....	31
2.1. Cells and Viruses.....	31
2.2. Liquid chromatography tandem mass spectrometry (LC-MS/MS) .....	32
2.3. qRT-PCR.....	33
2.4. Small-molecule inhibition .....	34
2.5. Immunoblotting .....	35
2.6. Plasmids and sgRNA Design .....	35
2.7. Lentivirus Production .....	36
Chapter 3: Results .....	38
3.1. HCMV induces CE biosynthesis .....	38
Introduction .....	38
Results .....	38
Discussion and Future Direction .....	45
3.2 Viral mechanisms of induced CE biosynthesis .....	48
Introduction .....	48
Results .....	48
Conclusions and future directions.....	51
3.3. The importance and implications of CE for HCMV replication .....	54

Introduction .....	54
Results .....	54
Conclusions and future direction .....	61
Chapter 4: Discussion .....	67
Chapter 5: References .....	74

## List of Figures and Tables

<b>Figure 1.</b> Schematic of HCMV remodeling of host metabolism to support lipid biosynthesis. ....	17
<b>Figure 2.</b> Structure of cholesteryl esters. ....	22
<b>Figure 3.</b> LC-MS/MS analysis of CE lipid detection between NH <sub>4</sub> and Na adducts. ....	39
<b>Figure 4.</b> CE are present in FBS. ....	40
<b>Figure 5.</b> HCMV-infected cells contain greater levels of CE lipids in fibroblast cells. ...	41
<b>Figure 6.</b> Characterizing CE population in uninfected HFF cells. ....	43
<b>Figure 7.</b> HCMV-infected cells contain greater CE lipids with LCFA- or VLCFA-tails ...	44
<b>Figure 8.</b> HCMV induces high CE accumulation through enhanced SOAT1 gene expression. ....	45
<b>Figure 9.</b> pUL37x1 is partially responsible for HCMV-mediated CE accumulation. ....	49
<b>Figure 10.</b> PERK suppresses HCMV-mediated CE accumulation. ....	51
<b>Figure 11.</b> Diagram of mechanism by which HCMV influences CE accumulation. ....	52
<b>Figure 12.</b> Avasimibe cytotoxicity in uninfected fibroblast cells. ....	55
<b>Figure 13.</b> Avasimibe reduces CE levels in HCMV-infected cells. ....	56
<b>Figure 14.</b> Avasimibe blocks HCMV viral replication. ....	57
<b>Figure 15.</b> Avasimibe treatment interferes with HCMV early protein expression. ....	58
<b>Figure 16.</b> Avasimibe treatment reduces HCMV viral DNA synthesis. ....	59
<b>Figure 17.</b> Avasimibe remains antiviral after treating HCMV-infected cells later during infection. ....	60
<b>Figure 18.</b> TMP-153 cytotoxicity in uninfected fibroblast cells. ....	61
<b>Figure 19.</b> TMP-153 reduces CE levels in HCMV-infected cells. ....	62
<b>Figure 20.</b> TMP-153 does not affect HCMV viral replication. ....	63
<b>Figure 21.</b> Diagram of SOAT1 inhibition and avasimibe's mechanism of antiviral activity. ....	64
<b>Figure 22.</b> Design and efficiency of CRISPR-mediated SOAT1 knockdown. ....	66
<b>Figure 23.</b> Possible pathways of PERK-mediated CE regulation during HCMV infection. ....	70

<b>Table 1.</b> Primer sequences used for qRT-PCR and qPCR analysis.....	33
<b>Table 2.</b> Antibodies used for western blot. ....	35
<b>Table 3.</b> sgRNA sequences used for developing CRISPR-knockout or CRISPRi- knockdown cells.....	36

## Abstract

Human cytomegalovirus (HCMV) is a  $\beta$ -herpesvirus that infects over 50% of people above the age of 40. Once infected, HCMV establishes a lifelong latent infection with periodic reactivation. Most infections are asymptomatic. However, infection in immunocompromised patients may result in fatal HCMV-related complications. Further, congenitally-acquired HCMV infection is the leading cause of birth defects in the United States. The HCMV virion contains a large double-stranded DNA genome encapsidated by a protein shell that is surrounded by a lipid membrane. Like all enveloped viruses, HCMV steals host lipids to generate its envelope membrane. While previous studies demonstrate that HCMV replication requires lipid metabolism, the details of virally-induced lipid changes remain poorly defined. We performed an untargeted lipidomic screen using liquid chromatography high resolution tandem mass spectrometry to identify and quantitatively measure how infection alters the lipidome of cells. We found that HCMV increases cholesteryl esters (CE) by 24 hours post infection. CE lipids are synthesized by sterol O-acyltransferase 1 (SOAT1) attaching a fatty acyl-CoA to a cholesterol molecule. I hypothesized that early stages of HCMV replication induce CE biosynthesis and that CE are required for viral replication. In support of our hypothesis, we found HCMV induces SOAT1 gene expression. Further, HCMV immediate early pUL37x1 is partially responsible for virally-induced CE accumulation. We found that treating infected cells with a SOAT1 inhibitor blocked CE production and infection. Overall, our findings suggest that HCMV induces CE synthesis that can be targeted to block infection.



# Chapter 1: Literature Review

## 1.1 Human Cytomegalovirus

Herpesviruses have a linear double-stranded DNA genome contained within an icosahedral capsid; a tegument layer composed of both viral- and host-derived molecules that are released into the cytoplasm upon cell entry; and a host-derived lipid envelope containing glycoproteins responsible for viral binding and entry into a cell<sup>1</sup>. The *Herpesviridea* family is composed of three subfamilies: alpha ( $\alpha$ )-, beta ( $\beta$ )-, and gamma ( $\gamma$ )-herpesviruses.  $\beta$ -herpesviruses, including human cytomegalovirus (HCMV, also known as human herpesvirus 5, HHV-5), show species specific host tropism but can infect a variety of cells within their host. Like all herpesviruses, HCMV establishes a lifelong persistent infection<sup>2</sup>. This chapter will focus on HCMV and its health implications, biology, and manipulation of cellular metabolism.

### Epidemiology and Health Implications

HCMV is prevalent throughout the global population, with an estimated 40-99% of the population seropositive<sup>3</sup>. The overall prevalence of HCMV in the United States is 59%, but age, race/ethnicity, and socioeconomic status impacts HCMV seroprevalence. More than 90% of people ages  $\geq 80$  years are infected, which is more than twice the infection rate among 6-11 year-olds<sup>4</sup>. In the United States, HCMV infection rates are also greater in African- and Mexican-American populations compared to non-Hispanic whites<sup>4</sup>. Additionally, HCMV infection is more common in populations of low socioeconomic status<sup>4</sup>.

Primary infection with HCMV establishes a lifelong latent infection, with periodic reactivation and shedding of virus<sup>3</sup>. HCMV can be acquired by contact with infectious bodily fluids, including saliva. The virus can be transmitted by sexual activity, blood transfusion, or organ transplantation<sup>5</sup>. The more common routes of acquiring HCMV include mother-to-child by breastfeeding, family-to-child by close contact, or at day care centers<sup>4</sup>. In addition to horizontal transmission (person to person), HCMV can undergo vertical transmission (mother to fetus)<sup>6</sup>.

While HCMV is typically asymptomatic in immunocompetent individuals, the pathology of immune-naïve cases can be extensive. Congenitally-acquired HCMV (congenital HCMV) is the leading cause of birth defects in the United States<sup>4</sup>. It is estimated that congenital HCMV occurs in 1 out of every 150 newborns<sup>2</sup>. Approximately 5-10% of congenital HCMV cases will be born with symptomatic disease, including visceral organomegaly, microcephaly, chorioretinitis, and skin lesions<sup>7</sup>. In addition, congenital HCMV can result in clinical consequences later in life. Children born with congenital HCMV are at risk for developing sensorineural hearing loss (SNHL), retinitis, mental retardation, microcephaly, seizures, and cerebral palsy<sup>3</sup>. SNHL is the most common consequence of congenital HCMV, with approximately 22-65% of children born with symptomatic disease and 6-23% of children with asymptomatic congenital HCMV infection developing SNHL<sup>8,9</sup>.

Previous epidemiological studies suggested that the greatest at-risk population for vertical transmission of HCMV is seronegative women of childbearing age. Approximately 30-50% of women of childbearing age are seronegative in industrialized nations<sup>4</sup>. It was estimated that congenital infection occurs in 20-50% of cases if the

mother experiences a primary infection while pregnant<sup>10</sup>. This was in stark contrast to women with preconceptional immunity to HCMV, where the rate of congenital infection drops to 0.1-2%<sup>10</sup>. While this suggests that maternal immunity is an important deterrent of HCMV from infecting the fetus, there are several untested assumptions that can skew our interpretations. First, it was assumed that congenital transmission of HCMV in women with preconceptional immunity was due to reactivation of latent HCMV<sup>11</sup>. One study in 1980 used restriction enzyme digestion to compare viruses between women and infants, which has limited capacity to distinguish distinct HCMV strains<sup>12</sup>. DNA sequencing of viral genes has become more commonplace in identifying HCMV strains and has indicated that immunocompetent individuals are capable of being infected with multiple unique strains of HCMV<sup>13</sup>. Furthermore, maternal reinfection with a distinct HCMV strain was associated with congenital acquisition of the newly acquired virus<sup>14,15</sup>. This suggests that existing immunity to HCMV does not prevent infection and congenital transmission with a new HCMV strain. Another assumption was that the rate of transmission between nonprimary vs primary HCMV infection during pregnancy is the same<sup>11</sup>. While studies have reported a 30% transmission rate among women who acquire HCMV during pregnancy, no studies have directly examined the rate of transmission in nonprimary infections during pregnancy<sup>16</sup>. Finally, the assumption that maternal preconception immunity can reduce HCMV-mediated fetal disease severity has limitations<sup>11</sup>. Since the frequency of severe medical complications occurs in 3-5% of all congenital HCMV infants, it is difficult to have adequate patient numbers to accurately test whether maternal immunity influences the severity of disease<sup>11</sup>.

Therefore, the notion that seronegative women of childbearing age are at the highest risk for congenital HCMV transmission is being revisited.

Despite the high prevalence of HCMV and its clinical consequences, many women of childbearing age are unaware of HCMV nor how to avoid infection during pregnancy<sup>17</sup>. Less than 1/5 of women are aware of HCMV; among women who have heard of HCMV, most have never heard of HCMV-related outcomes and how to prevent infection<sup>4</sup>. One reason for limited awareness is the lack of counseling by OB/GYNs about HCMV prevention, where less than half of OB/GYNs inform patients about HCMV<sup>4</sup>. One survey found that seronegative pregnant women are receptive to HCMV preventative counseling: there was an 84% reduction in seroconversion among pregnant woman caring for young children who received basic counseling on HCMV prevention relative to the comparison group<sup>18</sup>. Therefore, it is recommended that congenital HCMV receive more public awareness.

HCMV is also a major contributor to life-threatening complications for immunocompromised patients, such as HIV/AIDS patients and allograft recipients<sup>10,19</sup>. HCMV was one of the first opportunistic pathogens observed among HIV/AIDS patients and was associated with organ failure of the gastrointestinal tract and the eyes<sup>10</sup>. HCMV pathogenesis within the gastrointestinal tract included focal colitis and chronic dysfunction of intestinal tract absorption<sup>10</sup>. Prior to the development of antiretroviral drugs, HCMV retinitis was reported in approximately 25% of patients with HIV and typically manifested during late stages of AIDS<sup>10</sup>. Inflammation results in the loss of retinal structure and, under severe conditions, blindness<sup>10</sup>.

Allograft recipients under immunosuppressive therapy are also at risk for HCMV-related health complications that differ from those seen in HIV/AIDS patients. HCMV disease manifestations is dependent on the organ<sup>19</sup>. Incidences of HCMV disease is 25% among kidney, heart, and liver transplant recipients<sup>19</sup>. However, HCMV disease instances increase to 50% in pancreas or kidney-pancreas transplant recipients<sup>10</sup>. Symptoms of HCMV disease in allograft recipients include fever, myalgia, leucopenia, thrombocytopenia, pneumonitis, esophagitis, and colitis<sup>10</sup>. Further, HCMV infection increases the risk of both acute and chronic allograft rejection<sup>20</sup>.

Antiviral therapies have been used to reduce HCMV infection and disease in congenitally infected infants, HIV/AIDS patients, and allograft recipients in the United States<sup>21</sup>. There are several approved antiviral prophylaxis treatments for HCMV infection: ganciclovir, valganciclovir, cidofovir, foscarnet, and letermovir<sup>22</sup>. While letermovir interferes with viral DNA synthesis termination and packaging into capsids, the remaining therapies target viral DNA polymerase and inhibit viral DNA synthesis/elongation following phosphorylation by the viral kinase UL97<sup>22</sup>. While these drugs are efficient HCMV treatments, toxic side-effects constrain the duration and intensity of antiviral therapies; it is estimated that ganciclovir-treated marrow transplant recipients are at twice the risk for developing neutropenia when compared to untreated patients<sup>21</sup>. Developing novel antiviral strategies with improved toxicity scores against HCMV could improve clinical outcomes, particularly in cases of ganciclovir-resistant HCMV infection<sup>10</sup>.

Finally, HCMV has been associated with glioblastoma and cardiovascular diseases, however no direct link between infection and disease causation has been

established<sup>23–26</sup>. Cobb *et al.* found that HCMV nucleic acids and proteins are present in a large percentage of malignant glioma tissue<sup>24</sup>. Meanwhile, Rahbar *et al.* found that glioblastoma patients with low-grade HCMV infection had a median survival that was 20 months longer than patients with high-grade infection<sup>27</sup>. Further, a retrospective analysis on glioblastoma patients with HCMV-positive tumors showed that 62% of patients who received valganciclovir, an anti-HCMV medication, survived after two years post-prognosis compared to 18% of control patients<sup>28</sup>. There are numerous biological effects induced by HCMV proteins that might present oncogenic features. For example, Price *et al.* show that HCMV increases STAT3 phosphorylation and cellular proliferation in patient-derived glioblastoma<sup>29</sup>. Murine CMV (MCMV), which specifically infects mice but not humans, similarly increased phosphorylated STAT3 in mice neural stem cells<sup>29</sup>. They used a genetic mouse model of glioma (Mut3 mice) and found that MCMV-infected Mut3 mice had a shorter survival rate when compared to mock- or herpes simplex virus (HSV-1)-infected Mut3 mice<sup>29</sup>. This suggests that CMV-mediated STAT3 phosphorylation might play oncogenic roles in glioma progression. While these studies suggest an association between HCMV and cancer, a direct link connecting HCMV as the cause of glioblastoma severity remains to be determined.

The relationship between HCMV and atherosclerosis is similarly elusive. HCMV antigens and DNA have been identified in atherosclerotic lesions<sup>25</sup>. Arterial wall endothelial cells are susceptible to HCMV infection, which can lead to inflammation and increase the risk of developing atherosclerosis<sup>26</sup>. However, it is difficult to examine the epidemiological relationship between atherosclerosis and HCMV due to high HCMV seroprevalence and the age of atherosclerotic onset. Perhaps more convincingly,

HCMV infection increases modified low-density lipoprotein (LDL) uptake in human smooth muscle cells (SMCs)<sup>30</sup>. Since one of the predominant hallmarks of atherosclerotic development is increased modified LDL uptake, this provides mechanistic evidence supporting HCMV as a risk for developing atherosclerosis.

## **Human Cytomegalovirus Biology**

The overall size of the HCMV virion is approximately 230nm in diameter<sup>31</sup>. In terms of genome size and coding capacity, HCMV is the largest virus known to infect humans, with a genomic size of ~235 kbp<sup>32,31</sup>. The genome encodes over 200 known genes and may contain over 500 genes in total<sup>33</sup>. HCMV gene expression is highly organized and occurs in a cascade-like series of events. Broadly speaking, immediate early (IE) genes are required for subsequent viral gene expression and overall efficiency of viral replication<sup>34</sup>; early gene expression is necessary for viral DNA replication<sup>35</sup>; and late genes, whose expression is dependent on viral DNA replication, encodes for viral proteins required for virion maturation<sup>36,37</sup>.

HCMV can infect a broad range of human cells, with the status of viral replication dependent on the cell type. HCMV lytic infection produces high viral titers and occurs in epithelial, endothelial, fibroblasts, and smooth muscle cells<sup>38</sup>. HCMV latency is characterized as dormancy, where the viral genome is maintained without producing new viral progeny yet has the capability of reactivating viral replication in response to cellular changes<sup>39-43</sup>. Cell models used to study HCMV latency include CD34<sup>+</sup> human progenitor cells (HPCs) and monocytes<sup>44-46</sup>. While HCMV is efficient in infecting many types of human cells, HCMV is unable to infect other species. Consequently, most of

our understanding of HCMV replication and host interactions come from studying the virus in the context of primary human cell in cell culture.

## Manipulation of Cellular Metabolism

HCMV hijacks host cellular metabolism to acquire the molecular building blocks and energy required for efficient viral replication (**Figure 1**). Within the first 24 h of replication, HCMV activates AMP-activated protein kinase (AMPK) via  $\text{Ca}^{2+}$ -calmodulin-dependent kinase kinase (CaMKK), which consequently upregulates glucose transporter GLUT4 to increase glucose uptake<sup>47,48</sup>. Glucose feeds into the glycolytic pathway, which supplies pyruvate for the TCA cycle<sup>49,50</sup>. Rather than continue through the TCA cycle, citrate is transported from the mitochondria into the cytoplasm and is broken back down into acetyl-CoA, the subunit for fatty acid and cholesterol biosynthesis<sup>49</sup>. In addition to citrate-derived acetyl-CoA, HCMV-infected cells can acquire additional acetyl-CoA by the non-enzymatic breakdown of pyruvate into acetate<sup>51</sup>.

HCMV uses acetyl-CoA for fatty acid synthesis by supporting acetyl-CoA carboxylase (ACC1) activity, which attaches a carboxyl group to acetyl-CoA to produce malonyl-CoA<sup>52</sup>. Both malonyl-CoA and acetyl-CoA are used by fatty acid synthase (FAS) to catalyze the synthesis of fatty acid species palmitoyl-CoA (C16:0)<sup>49</sup>. Palmitoyl-CoA can be elongated by fatty acid elongases (ELOVLs), which uses malonyl-CoA to further extend the growing fatty acyl-CoA by two carbon units per reaction<sup>53,54</sup>. HCMV virion release and infectivity depends on the synthesis and incorporation of saturated very long chain fatty acid (VLCFA) lipids into the viral envelope<sup>53,54</sup>. By 48 h post



infection, HCMV-infected cells have a ~3.5-fold increase in lipid synthesis compared to uninfected cells<sup>55,56</sup>.

HCMV similarly requires acetyl-CoA as a subunit for cholesterol biosynthesis. 3-hydroxy-3-methyl-glutaryl-CoA reductase (HMGCR) is the rate-limiting enzyme of the mevalonate pathway, which produces cholesterol and other isoprene metabolites. HCMV-mediated activation of sterol regulatory element binding protein (SREBP) induces HMGCR gene expression by 5-fold<sup>55</sup>. Cholesterol is incorporated into the viral

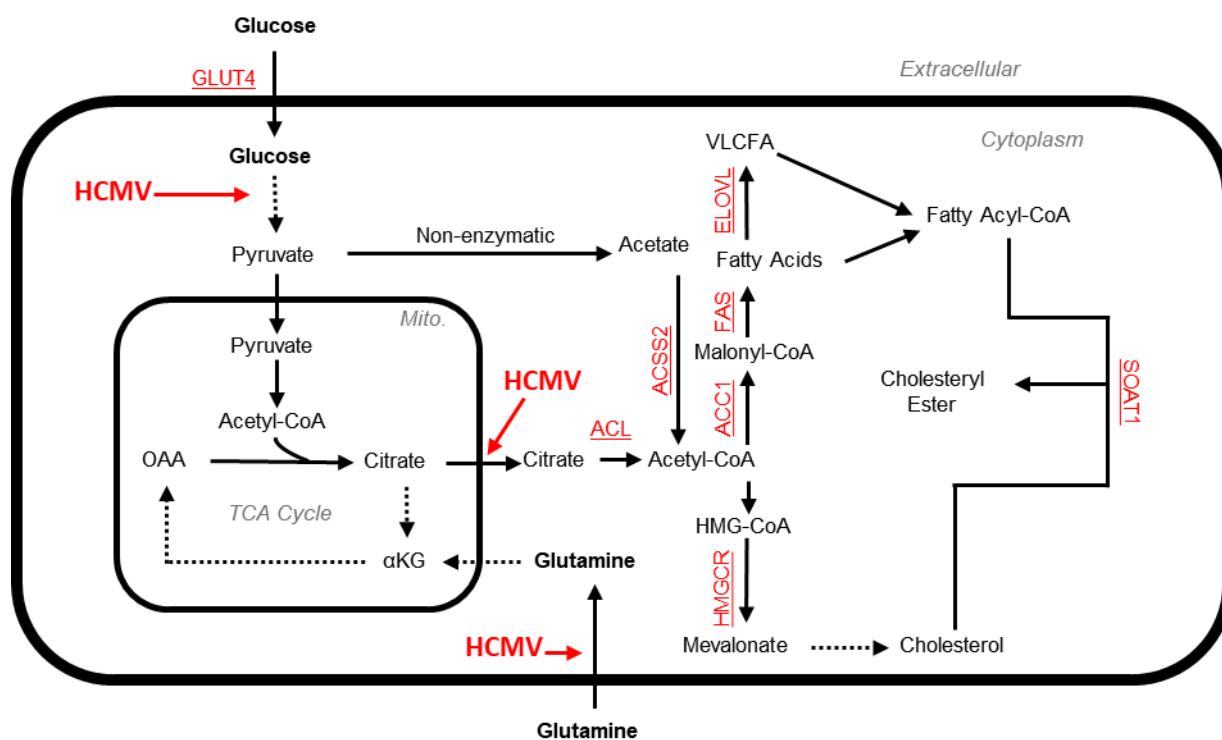


**Figure 1. Schematic of HCMV remodeling of host metabolism to support lipid biosynthesis.**

Glucose and glutamine metabolism contributes to fatty acid and cholesterol synthesis in HCMV-infected cells. Enzymes underlined in red are associated with the fatty acid and mevalonate pathways, which are upregulated by HCMV. The dashed line connecting glucose to pyruvate represents glycolysis. The dashed lines in the mitochondria represent the TCA cycle. The dashed line connecting mevalonate to cholesterol represents the mevalonate pathway. Abbreviation: AMPK, AMP-activated protein kinase; GLUT4, glucose transporter 4;  $\alpha$ KG,  $\alpha$ -ketoglutarate; Mito., mitochondrion; TCA, tricarboxylic acid; ACSS2, acetyl-CoA synthetase short-chain family member 2; ACL, ATP-citrate lyase; ACC, acetyl-CoA carboxylase; FAS, fatty acid synthase; HMG, 3-hydroxy-3-methylglutaryl; HMGCR, HMG-CoA reductase; ELOVL, elongase; SOAT1, sterol O-acyltransferase 1.

envelope and supports infectivity by promoting fusion of the viral envelope with the cell membrane<sup>57</sup>. In response to infection, cells limit cholesterol availability by expressing greater surface levels of low density lipoprotein related receptor 1 (LRP1) to limit HCMV replication<sup>57</sup>. This further demonstrates the necessity of cholesterol to HCMV infection.

To meet an increase demand for lipids, HCMV activates the lipogenic transcription factors SREBPs and carbohydrate regulatory element binding proteins (ChREBPs) by 24 and 48 hpi, respectively<sup>55,56</sup>. In cholesterol-rich states, inactive SREBPs are anchored to the ER membrane as a complex with SREBP cleavage activation protein (SCAP) and insulin-induced gene 1 (Insig-1)<sup>58</sup>. The SREBP-SCAP-Insig complex is mediated by ER-resident sterol concentration. When sterol levels are low, SREBP-SCAP dissociate from Insig-1 and translocate to the Golgi. Protease enzymes S1P and S2P cleave SREBP, allowing its translocation to the nucleus and induction of lipogenic enzyme expression. HCMV-mediated activation of SREBP1 leads to increased expression of lipogenic enzymes ACC1, ATP citrate lyase (ACL), FAS, HMGCR, and sterol CoA desaturase 1 (SCD1)<sup>55</sup>.

While SREBPs respond to sterol levels, ChREBPs are regulated by glucose signaling<sup>59</sup>. Glucose can be converted to xylulose-5-phosphate via the non-oxidative phase of the pentose phosphate pathway, which can activate protein phosphatase 2A (PP2A). PP2A dephosphorylates ChREBP, allowing ChREBP to enter the nucleus<sup>59</sup>. Another PP2A-mediated dephosphorylation event permits ChREBP to bind to carbohydrate responsive elements and promote glycolytic and lipogenic gene expression<sup>59</sup>. HCMV-mediated ChREBP activation increases the expression of ACC1, ACL, FAS, and ELOVL6<sup>56</sup>. shRNA-mediated inhibition of either SREBP1 or ChREBP1

activation reduces HCMV-mediated lipid and viral replication<sup>55,56</sup>. Thus, HCMV relies on the activation of SREBPs and ChREBPs for sufficient lipid biosynthesis.

HCMV-induced lipid metabolism also requires ER-membrane associated sensor protein PKR-like ER kinase (PERK)<sup>60,61</sup>. In non-stressed conditions, PERK is bound to the ER by chaperone immunoglobulin heavy-chain-binding protein (BiP). When unfolded proteins accumulate in the ER, BiP dissociates from PERK, allowing PERK to homodimerize and autophosphorylate. Activated PERK phosphorylates eukaryotic initiation factor 2 $\alpha$  (eIF2 $\alpha$ ) to attenuate protein translation. However, during the unfolded-protein response eIF2 $\alpha$  promotes the translation of activating transcription factor 4 (ATF4). ATF4 increases the expression of metabolic and redox regulatory genes that will assist in ER-stress resolution<sup>60,62</sup>. Further, PERK regulates lipid biogenesis by activating SREBP1 in addition to other possible mechanisms<sup>62,63</sup>. HCMV induces PERK expression by 24 hpi, supporting SREBP1 activation and elevated lipid synthesis while simultaneously interfering with PERK-mediated inhibition of translation<sup>60,61</sup>.

HCMV similarly activates the mammalian target of rapamycin (mTOR), which subsequently increases active SREBP1<sup>55</sup>. HCMV's early protein pUL38 keeps mTOR in an active state by antagonizing its inhibitor, the tuberous sclerosis protein complex (TSC1/2)<sup>64</sup>. pUL38-mediated mTOR activity increases SREBP1 maturation and saturated very long chain fatty acid (VLCFA) elongation. mTOR activity ensures that saturated VLCFAs are incorporated into the viral envelope, allowing the release of HCMV virions<sup>53,54</sup>. Further, mTOR activates peroxisome proliferator-activated receptor gamma (PPAR $\gamma$ )<sup>65</sup>. PPARs are nuclear receptors that regulate fatty acid storage and

glucose metabolism<sup>66</sup>. In human neural progenitor cells, HCMV strongly increases PPAR $\gamma$  expression and activity<sup>67</sup>. Although the role of PPAR $\gamma$  in HCMV is poorly defined, several studies in adipocytes have shown that rapamycin inhibition of mTORC1 reduces PPAR $\gamma$  expression and activity<sup>68,69</sup>. In summary, PPAR-control of lipid metabolism may be important to HCMV infection, but needs further studies.

The focus of our lab is to examine the role of lipid metabolism for HCMV replication. Since my project focuses on HCMV-induced changes in cholesteryl ester (CE) metabolism, I will focus on CE in the following literature review section.

## 1.2. Cholesteryl Esters

Lipids are hydrophobic or amphipathic hydrocarbon molecules that provide many essential functions. The function of lipids includes: being a structural unit for all cellular membranes, energy storage, and signaling messengers. Lipids typically consist of a headgroup and one-three fatty acid tails that are connected by a glycerol backbone<sup>70</sup>. The type of headgroup and tails dictates the function of the lipid, such as the capacity to associate into a lipid bilayer. Various molecules can be used as headgroups, e.g. a modified phosphate-group or a sugar group. Cholesterol can also serve as a headgroup; in this case, there is no glycerol backbone. The hydrocarbon tails can have varying lengths (i.e. number of carbons) and degree of unsaturation (i.e. number and location of carbon-carbon double bonds). Furthermore, the lipid-tail bonds can vary. For example, phosphatidylcholine lipids contains a phosphocholine headgroup connected to a glycerol backbone that has two tails connected by ester bonds, whereas plasmalogens contain the same headgroup with one of its tail attached to the glycerol

backbone via an ether linkage<sup>70</sup>. By varying the combination of headgroups and tails, a cell can produce a lipidome with a large range of diversity that can perform numerous biological functions.

Lipid nomenclature is based on the headgroups, followed by tail chain length and degree of unsaturation<sup>70</sup>. For example, CE (18:1) represents a cholesteryl ester lipid, with a cholesterol molecule serving as the headgroup and a mono-unsaturated (i.e. one double bond) fatty acid tail that is 18 carbons long.

Sterol lipids have diverse biological functions. One sterol subcategory includes cholesterol and its derivatives, which are important for membrane fluidity and energy storage<sup>71</sup>. Cholesteryl esters are categorized as a derivative of cholesterol, which will be the focus of this section.

## Structure and function

Cholesteryl esters (CE) are neutral lipids (i.e. no charged head group) that are composed of a sterol headgroup and one fatty acid tail (**Figure 2**). These lipids are formed from an ester bond between the hydroxyl group of cholesterol and the carboxylate group from a fatty acyl-CoA. CEs accumulate within the neutral core of lipid droplets and lipoproteins.

The main function of CE lipids is to act as a storage unit for cholesterol and fatty acids. In nutrient-limiting conditions, cells can generate energy by breaking down stored CE<sup>72</sup>. CE lipids are also important for intracellular cholesterol homeostasis since excessive cholesterol can be stored as CE until needed<sup>73,74,75</sup>.

In humans, CE are also important for the transportation of cholesterol and fatty acids. Extracellular transport of neutral lipids is accomplished by a macromolecular assembly called lipoproteins. Lipoproteins exist as multiple classes that can be distinguished by density and carrier proteins called apolipoproteins. Lipoproteins allow for the distribution of diet-derived CE from the intestines to either the liver, where they will be stored, or to other tissues that require cholesterol<sup>76</sup>.

### Cellular acquisition of CE

A cell can acquire CE lipids is by lipoprotein import. Lipoproteins facilitate the transportation of diet-derived CE from the intestines to the target tissues, where they can be consumed or stored<sup>76</sup>. Lipoproteins can be categorized into several classes based on point-of-synthesis, lipid composition, and apolipoprotein content. Different lipoproteins contain varying levels of CE, with the most CE abundance found in low-density lipoproteins (LDL) and the least in chylomicrons. Apolipoproteins, which are

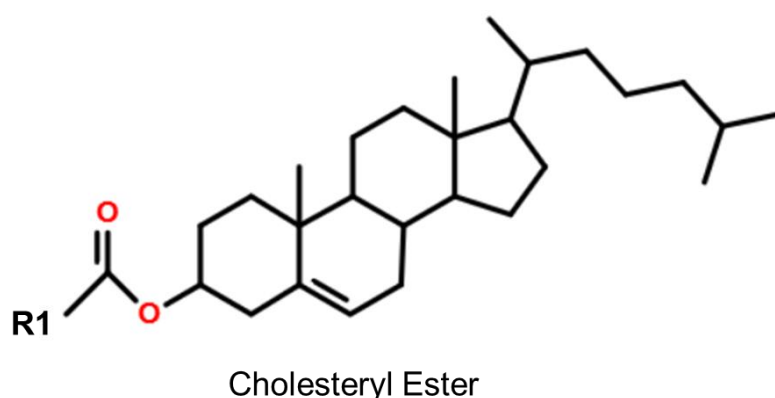


**Figure 2. Structure of cholesteryl esters.**

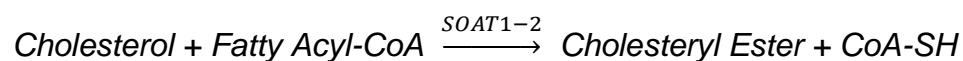
CE lipids are composed of a cholesterol headgroup attached to a fatty acid tail (R1) by an ester bond. CE fatty acid tails can vary by carbon length and degree of unsaturation.

present on the surface of lipoproteins, are responsible for transportation and interactions with enzymes, transfer proteins, transmembrane transporters, and cell surface receptors<sup>77</sup>. ApoB-100 is solely found on LDL, which carry the most free-cholesterol and CE. LDL are endocytosed by apoB-100-mediated binding to LDL receptors<sup>78,79</sup>. Once internalized, LDL is delivered to the lysosome and undergoes hydrolysis, releasing CE-derived cholesterol<sup>79</sup>.

Alternatively, CE can be produced by *de novo* biosynthesis. There are distinct enzymes that are responsible for producing CE. Lecithin:cholesterol acyltransferase (LCAT), a soluble plasma enzyme, is responsible for transferring a fatty acyl-tail from a phosphatidylcholine (PC) lipid onto a cholesterol molecule to produce CE on the surface of high-density lipoproteins (HDLs)<sup>80</sup>. Alternatively, intracellular CE biosynthesis is mediated by sterol O-acyl transferase (SOAT, also known as acyl-CoA:cholesterol acyltransferases [ACAT]). SOAT (ACAT) are the focus of the next section.

### **Sterol O-Acyltransferases 1-2**

Mammals express two SOAT enzymes from independent genes: SOAT1 and SOAT2. Both SOAT enzymes are members of the membrane-bound O-acyltransferase (MBOAT) family of enzymes, which catalyze the transfer of a fatty acyl-CoA onto the hydroxyl group of a specific hydrophobic molecule.<sup>81</sup> SOAT1-2 rely on cholesterol as the hydroxyl-containing hydrophobic molecule to produce CE. SOAT1-2 catalyzes:



SOAT1 is expressed in most tissues, localizes to the ER, and regulates intracellular cholesterol homeostasis<sup>82,83</sup>. SOAT2, on the other hand, is mostly expressed in the intestines and hepatocytes. SOAT2 converts diet-derived cholesterol and fatty acyl-CoA into CE for lipoprotein packaging and transport<sup>81,84</sup>.

The human *Soat1* gene is located on two chromosomes, 1 and 7, which possess independent promoters from one another (P1 and P7). Northern blot analysis indicate that four *Soat1* mRNAs exist (7.0, 4.3, 3.6, and 2.8 kbp), which all share the same 5'-untranslated region and coding sequence, yet differ in the length of untranslated regions<sup>85</sup>. While most *Soat1* mRNA is derived from chromosome 1, the 4.3-kbp mRNA is produced by both chromosomes 1 and 7, potentially by trans-splicing two precursor RNAs<sup>85</sup>. Expression of the *Soat1* gene on chromosome 1 yields the typical SOAT1 protein (50kDa). The chimeric *Soat1* mRNA encodes for a 56-kDa protein with approximately 30% of the enzymatic activity of the 50-kDa protein<sup>86</sup>. While the significance of this finding remains unclear, it is possible that the 56-kDa protein acts as an endogenous inhibitor of the 50-kDa protein activity<sup>86</sup>. Further research is required to elucidate the importance of both SOAT1 proteins.

In humans, *Soat2* is located on chromosome 12 and encodes for a 49kDa protein<sup>87</sup>. *Soat2* gene expression is regulated by the transcription factors Cdx2 and HNF1 $\alpha$ <sup>88</sup>. While HNF1 $\alpha$  is expressed in a range of tissues (hepatocytes, pancreas, kidney, stomach, and intestines), Cdx2 is specifically expressed in the intestines. This suggests that Cdx2 is responsible for SOAT2-specific tissue tropism. Unlike most lipogenic enzymes, neither SOAT1-2 have been shown to be transcriptionally regulated by SREBPs<sup>83</sup>.



Both SOAT1 and SOAT2 are allosteric enzymes that are activated by cholesterol<sup>89</sup>. One study proposes that SOATs contains both an activation site and a substrate site<sup>90</sup>. Rogers *et al.* show that the presence of cholesterol increased the SOAT-mediated esterification of pregnenolone (PREG), a sterol molecule. However, removing cholesterol reduced PREG esterification despite PREG having a stronger binding affinity for SOAT1 than cholesterol. This suggests that 1) PREG is a substrate but not an activator, 2) cholesterol is both a substrate and an activator, and 3) there are two distinct sterol binding sites: one for the activator and another for the substrate<sup>90</sup>.

### **Roles of SOAT in metabolic diseases**

CE metabolism has long been linked to the development of atherosclerosis. Early stages of disease are characterized by chronic inflammation and dyslipidemia, where high levels of cholesterols, neutral lipids, and lipoproteins are present in the plasma<sup>91</sup>. These conditions lead to monocyte adherence to inflamed endothelium and incorporation into the artery, where they will differentiate into macrophages and endocytose oxidized LDL (ox-LDL) via the scavenger receptor. Ultimately, excess incorporation of cholesterol from ox-LDL and SOAT1-mediated CE biosynthesis leads to a large accumulation of lipid droplets and the development of a 'foamy' phenotype<sup>91</sup>. Macrophage- and SMC-derived foam cell accumulation at atherosclerotic plaques increase the risk of plaque rupture and blockage of the artery lumen<sup>92</sup>. One study found that SOAT1 overexpression induced high CE accumulation and foam cell formation<sup>93</sup>. Accad *et al.* used mice deficient in either apoE or LDL receptor to induce severe hypercholesterolemia to study the effects of SOAT1<sup>-/-</sup> during the development of

atherosclerosis<sup>94</sup>. SOAT1 deficiency did not prevent atherosclerotic lesion development but did change the composition of the lesions by reducing neutral lipids and resident macrophages<sup>94</sup>. Despite these promising phenotypes, SOAT1 deficiency markedly interfered with cholesterol homeostasis that lead to severe hyperlipidemia<sup>94</sup>. This study was further supported by the findings of Yagyu *et al.*, who found that SOAT1-specific knockdown in tissue macrophages protects against CE accumulation but then promotes cutaneous xanthomatosis, or the accumulation of yellowish fatty material that can be observed as skin lesions<sup>95</sup>. These studies demonstrate the role of SOAT1 in cholesterol homeostasis and the caution that should be taken when developing therapies against atherosclerosis.

As previously discussed, HCMV might be a co-factor for atherosclerosis<sup>96</sup>. For example, HCMV genomic DNA has been identified in the wall of atherosclerotic vessels and transplant recipients who received hearts from HCMV positive donors are at a higher risk of developing accelerated coronary atherosclerosis than from HCMV-negative donors<sup>97,98</sup>. HCMV has also been found to increase the uptake of ox-LDL by increasing class A scavenger receptor gene expression in human aortic SMCs, an important characteristic in macrophage and SMC-derived foam cells<sup>30</sup>. The parallel between HCMV-mediated lipid biosynthesis in SMCs and the high-lipid accumulation found in atherosclerotic lesions supports speculations of HCMV as a co-factor for atherosclerosis. Additional research is required to define the mechanism behind HCMV-mediated CE accumulation in atherosclerosis.

Cancer cells manipulate metabolic pathways to support rapid oncogenic growth, including enhanced glycolysis, biosynthesis of macromolecules, and *de novo* lipid

biosynthesis<sup>99,100,101</sup>. Lipid droplet accumulation occurs in numerous cancers including glioblastoma, breast, colon, prostate, and pancreatic cancer<sup>102,103,104,41,42,43</sup>. Geng *et al.* found that SOAT1 is highly expressed in glioblastoma and is responsible for maintaining SREBP1 activation<sup>102</sup>. Yue *et al.* similarly contributed SOAT1-mediated CE accumulation in prostate cancer as being critical for promoting the expression and activation of SREBP1 and LDL receptors<sup>106</sup>. In addition, one study found that aggressive human prostate cancer induces the PI3K/AKT/mTOR pathway, which is required for high expression of SOAT1 and aggressive CE accumulation<sup>106</sup>. Li *et al.* similarly found that metastatic pancreatic cancer increases SOAT1-mediated CE accumulation to maintain high metabolic activity and to remove the cytotoxic effects of excess cholesterol<sup>107</sup>. Together, these studies suggest a variety of cancers use a similar method of maintaining high lipid metabolism by upregulating SOAT1 activity to remove free cholesterol that would otherwise interfere with SREPB and LDL receptor activation. Since HCMV is speculated to be a oncomodulator, studying the role of virus-mediated CE metabolism could reveal molecular mechanisms responsible for oncogenesis<sup>24,108–110</sup>.

### **Manipulation of CE by viruses**

Herpesviruses rely on host lipid metabolism to replicate. One of the first reports of herpes-induced CE accumulation was in 1981 by Fabricant *et al.*, who identified a 3-6-fold increase in cholesterol and CE accumulation in cultured arterial SMCs infected with Marek's disease herpesvirus (MDV), an alphaherpesvirus that infects chickens<sup>111</sup>. Specifically, MDV induces high CE accumulation by decreasing the rate of CE

hydrolysis via inhibition of neutral cholesteryl esterase (NEH) activity, increased cholesterol biosynthesis, reduced cholesterol excretion, and increased SOAT activity<sup>112</sup>. It was later determined that HSV-1 similarly induces high CE and triacylglycerol accumulation in arterial SMCs, partially as a result of reduced CE hydrolysis<sup>113</sup>. While these observations show herpesviruses induce high CE accumulation, the purpose of CE metabolism during infection remains unclear. While we know herpesvirus infection reduces CE hydrolysis while increasing SOAT activity, it remains unclear whether this phenomenon is virus-mediated hijacking or a host cellular response to infection.

Low *et al.* found HCMV did not induce CE lipid accumulation, despite greater incorporation of [<sup>4</sup>C] oleic acid into CE<sup>114</sup>. They attributed [<sup>4</sup>C] oleic acid incorporation into CE to HCMV protein US28, a G-protein-coupled receptor that is expressed throughout viral replication<sup>114</sup>. Nonetheless, Low *et al.* claimed that US28-transfected cells had similar CE concentrations as mock cells<sup>114</sup>. However, their fibroblast cells were infected in the presence of FBS. It is possible that the discrepancy between Low *et al.* and our results is due to the lipids present in FBS; our LC-MS/MS results indicate that CE are present in FBS and could serve as an exogenous source (as discussed below in the result section). Importantly, Low *et al.* normalized lipid composition to phosphatidylcholine, a phospholipid that we found is dramatically greater in HCMV-infected cells (Purdy lab unpublished). This likely led to misinterpretations of their observations. In the following chapters, I demonstrate that HCMV induces SOAT1 gene expression and dramatically increases CE lipids. Further, I will show that treating cells with avasimibe, an inhibitor of SOAT1, limits HCMV induction of CE synthesis and blocks virus replication.

One of the most characterized viruses that manipulate CE metabolism is hepatitis C virus (HCV)<sup>115-118</sup>. HCV is a member of the *Flaviviridae* family, which also includes Dengue virus (DENV), West Nile virus (WNV), and Zika virus (ZIKV). It is estimated that 75-85% of HCV cases develop into chronic infections, where 10-20% will develop liver injury, fibrosis, cirrhosis, or hepatocellular carcinoma<sup>119</sup>. One meta-analysis found that the overall prevalence of hepatic steatosis in chronic HCV infections was approximately 69%, which is two-fold higher than the general population<sup>120</sup>. This phenomenon is suggestive of HCV-mediated induction of lipid droplet accumulation within hepatocytes.

HCV replication depends on lipid metabolism. HCV virions use LDL receptors and HDL receptor scavenger class B type I to promote viral binding and entry<sup>121,122</sup>. Expression of viral protein NS4B induces the formation of an ER-derived membranous web while viral protein core interacts with lipid droplets, leading to the localization of lipid droplets in proximity to the membranous web. Once established, the lipid droplet-containing membranous web serves as the site of viral replication and virion assembly<sup>123</sup>. HCV eventually uses cellular lipoprotein assembly for egress, emerging as a lipoviral particle containing apoB, apoE, and apoC1<sup>124</sup>.

A lipidomic profile of purified HCV virions found that CE compose of 44% of total virion lipids, suggesting that high CE accumulation is important for virion maturation<sup>117</sup>. Indeed, one study showed that HCV induces high SOAT1 and SOAT2 gene expression in Huh7 cells and that SOAT-mediated CE are important for lipoviral infectivity<sup>115</sup>. Further, Hu *et al.* showed that treating HCV-infected cells with the SOAT1-2 small-molecule inhibitor avasimibe significantly reduced viral assembly<sup>116</sup>. However, they

contributed avasimibe's antiviral capacity to its off-target downregulation of microsomal triglyceride transfer protein (MTTP) expression<sup>116</sup>. MTTP, which transfers triglycerides to lipoproteins, is critical for the initial steps of VLDL and chylomicron assembly in the liver and intestines<sup>116</sup>. While Hu *et al.* suggests that HCV replication is more dependent on MTTP, Read *et al.* show that SOAT inhibition by TMP-153 reduces virion infectivity<sup>115</sup>. Since CE lipids make up the majority of HCV lipoviral particles, inhibition of *de novo* CE biosynthesis increased the density of lipoviral particles while making them less infectious<sup>115</sup>. Together, this suggests that HCV replication depends on both CE biosynthesis and MTTP-mediated lipoprotein assembly for viral maturation and infectivity. As Hu *et al.* showed, small-molecule inhibitors can have off-target effects that can skew our interpretations if not further investigated. Developing a SOAT knockout model could provide more direct evidence on the role of SOAT1-2 in HCV replication.

The focus of this study is to examine the role of CE lipid metabolism during HCMV replication. We initially found that HCMV-infected cells contain high CE accumulation and SOAT1 gene expression by 24 hpi. Therefore, we hypothesized that early stages of HCMV replication promote CE biosynthesis and that this pathway can be targeted to block viral replication. The goals of this project include: 1) characterizing CE lipid biosynthesis in HCMV-infected cells; 2) identifying viral mechanisms of inducing CE accumulation; and 3) testing whether CE biosynthesis is important for viral replication.

## Chapter 2: Materials and Methods

### 2.1. Cells and Viruses

Low-passage human foreskin fibroblasts (HFF; ATCC), life-extended HFF (HFF-hTERT), and 293FT cells were cultured in Dulbecco modified Eagle medium (DMEM; 4.5 g/L glucose and L-glutamine) supplemented with 10% fetal bovine serum (FBS), HEPES, and penicillin/streptomycin. Primary HFF-dCas9 cells were maintained in DMEM supplemented with 2 $\mu$ g/mL doxycycline to induce dCas9-KRAB expression.

The HCMV AD169-GFP strain was used throughout this study. Our AD169-GFP virus stocks were generated from a bacteria artificial chromosome (BAC) that contains the AD169 genome with a SV40 early promoter-driven GFP gene inserted in place of the nonessential UL21.5 gene<sup>125,126</sup>. *Bads<sub>sub</sub>UL37x1*, a mutant virus derived from the AD169 BAC, was developed via allelic exchange<sup>125,127</sup>. The *Bads<sub>sub</sub>UL37x1* mutant virus was kindly provided by Dr. Thomas Shenk. To prepare virus stocks, we layered supernatant from infected HFF cells over 20% sorbitol and pelleted the virus by centrifugation (20,000 rpm, 1 h, room temperature)<sup>128</sup>. We prepared virus stocks in serum-free DMEM to prevent serum stimulation of HFF cells during viral inoculation<sup>128</sup>. Unless otherwise stated, experiments were performed in HFF cells that were maintained at confluence for 3 days and switched to DMEM without FBS for 1 day before infection. These cellular conditions have been widely used to study HCMV metabolic remodeling<sup>47–50,54–56,61,128–131</sup>. In addition, we avoided adding FBS to our infection experiments because of the presence of exogenous CE lipids that might

otherwise interfere with our results (**Figure 4**). We measured virus production from infected cells by using the 50% tissue culture infective dose (TCID<sub>50</sub>) method.

## **2.2. Liquid chromatography tandem mass spectrometry (LC-MS/MS)**

All lipid extraction experiments were performed in 6-well plates. Experimental conditions were tested using three wells, with two wells used as duplicates for LC-MS/MS analysis and the third well used to count cells for lipid resuspension. Prior to lipid extraction, cells were washed with PBS and the metabolic reactions in cells were rapidly halted by the addition of cold (-20°C) 50% methanol containing 0.1M HCl. The cells were scraped and transferred to glass vials. All subsequent steps were performed in glass vials using glass syringes. Lipids were extracted by adding chloroform, vigorously vortexing, and centrifuging (1,000 x g, 10 min, 4°C). Once the lipid-containing chloroform was extracted, samples were dried under N<sub>2</sub> gas and resuspended in 1:1:1 chloroform:methanol:isopropanol (100µL resuspension solution per 2.0 x 10<sup>5</sup> cells). CE lipids were analyzed by liquid-chromatography tandem high-resolution mass spectrometry (LC-MS/MS) using a Q-Exactive Plus orbitrap mass spectrometer (Thermo). CE lipids were identified and quantitatively measured in positive mode with electrospray ionization. Samples were run on a C18 reverse-phase column (Phenomemex) on a gradient from buffer A (60% methanol with 10mM ammonium formate and 0.1% formic acid) to buffer B (10% methanol and 90% isopropyl alcohol with 10mM ammonium formate and 0.1% formic acid) during a 30-min run time. MS data was analyzed using MAVEN: Metabolomic Analysis and Visualization Engine<sup>132,133</sup>.



CE identification was confirmed by identifying the stable and conserved cholestene fragment ( $m/z$  369.3516) using high-energy collisional dissociation MS/MS<sup>134</sup>.

### 2.3. qRT-PCR and qPCR

Transcriptional gene expression was examined by quantitative reverse transcription polymerase chain reaction (qRT-PCR). RNA samples were extracted using the Quick-RNA Miniprep kit (Zymo Research) according to the manufacturer's protocol. mRNA was converted to cDNA by reverse transcription using an anchored-oligo dT primer and 500ng total RNA (using the Transcriptor First Strand cDNA Synthesis kit from Roche). We measured cDNA levels by real-time qPCR using SYBR Green (Fisher). The sequence of primers used are listed in **Table 1**.

The accumulation of viral genome was examined by qPCR. DNA samples were extracted using the Quick-DNA Miniprep kit (Zymo Research) according to the manufacturer's protocol. Cellular and viral genomes were quantified using primers against  $\beta$ -actin and UL123, respectively. The sequences of primers used are listed in **Table 1**.

**Table 1. Primer sequences used for qRT-PCR and qPCR analysis.**

qPCR Primer Set	Forward Primer	Reverse Primer
H6PD	GGACCATTACTTAGGCAAGCA	CACGGTCTCTTTCATGATGATCT
Actin	TCCTCCTGAGCGCAAGTACTC	CGGACTCGTCATACTCCTGCTT
SOAT1	CCACTGGTCCAGATGAGTTTAG	GGGAACATGCAGAGTACCTTT
SOAT2 Set 1	GTCTTTGCCAACATGAGCCG	CCACCAGTCCCGGTAGAACA
SOAT2 Set 2	GCATGGAACGTGCTGATGTG	AGAAAGTTGCCTGGGGTAAGG
SOAT2 Set 3	ATGGAACGTGCTGATGTGGACCAT	TCAGTCCTTGCACATTCCTTGGTG
UL123	GCCTTCCCTAAGACCACCAAT	ATTTTCTGGGCATAAGCCATAATC

## 2.4. Small-molecule inhibition

Avasimibe (CI-1011; PD 148515; [[2,4,6-tris(1-methylethyl)phenyl]acetyl]-,2,6-bis(1-methylethyl)phenyl ester] sulfamic acid) was purchased from Sigma-Aldrich. TMP-153 (N-[4-(2-chlorophenyl)-6,7-dimethyl-3-quinolinyl]-N'-(2,4-difluorophenyl)-urea) was purchased from Cayman Chemicals. Stock solutions of avasimibe and TMP-153 were prepared in DMSO.

Cell viability after 96 h treatment with either avasimibe or TMP-153 was assessed by the CellTiter 96 AQueous One Solution assay (Promega). HFF cells were plated at a density of 8,000 cells per well in 100 $\mu$ L DMEM on 96-well plates. Unless otherwise stated, cells were maintained at confluency for 3d and switched to DMEM without FBS for 1 day before treatment. When treating cells, the medium was replaced with DMEM containing either DMSO (0.125% vol/vol when testing avasimibe; 0.05% vol/vol when examining TMP-153) as a control or increasing concentrations of drug. The medium with avasimibe or TMP-153 was replenished at 48 h post treatment and cell viability was measured at 96 h post treatment.

To assess HCMV infectivity in the presence of avasimibe or TMP-153, cells were infected at a multiplicity of 3 IU/cell. After a 1 h infection period, the cells were washed with PBS and then provided growth medium containing drug or DMSO alone. Again, the medium with avasimibe or TMP-153 was replenished at 48 h post infection.

## 2.5. Immunoblotting

Host and viral proteins were examined by western blot. Protein lysates were separated by SDS-PAGE and transferred onto a nitrocellulose membrane prior to blocking with either 3% BSA or 1% milk in tris-buffered saline containing 0.1% Tween 20. Primary antibodies used in this study are listed in **Table 2**. Fluorescent secondary antibodies were used to image the blot on an Odyssey CLx imaging system (Li-Cor).

**Table 2. Antibodies used for western blot.**

Antigen	Supplier/Citation	Catalog No. or clone	Antibody Species	Use
pUL26 <sup>135</sup>	Munger et al., 2006	7H1-5	Mouse	1:150 in 3% BSA for 1h
pUL37x1 <sup>127</sup>	Sharon-Friling et al. 2006	4B6-B	Mouse	1:50 in 3% BSA for 1h
pUL44	Virusys	CA0006-100	Mouse	1:1,000 in 3% BSA for 1h
pUL82 <sup>136</sup>	Kalejta et al., 2003	2H10-9	Mouse	1:150 in 3% BSA for 1h
pUL99 <sup>137</sup>	Silva et al., 2003	10B4-29	Mouse	1:150 in 3% BSA for 1h
pUL123 (IE1) <sup>138</sup>	Zhu et al., 1995	IB12	Mouse	1:100 in 3% BSA overnight at 4°C
PERK	Cell Signaling	3192S	Rabbit	1:600 in 1% milk overnight at 4°C
Tubulin	Sigma	T6199-200UL	Mouse	1:2,000 in 3% BSA for 1h

## 2.6. Plasmids and sgRNA Design

We developed our HFF-hTERT Cas9 CRISPR cells using the lentiCRISPR v2 plasmid (Addgene plasmid #52961)<sup>139</sup>. To develop HFF-dCas9 CRISPR interference (CRISPRi) cells, we used the doxycycline-inducible pHAGE TRE dCas9-KRAB plasmid (Addgene plasmid #50917)<sup>140</sup>. For SOAT1 sgRNA plasmid construction, we used pLenti SpBsmBI sgRNA Hygro, a pLKO.1 plasmid with hygromycin resistance and an oligonucleotide cloning site containing two BsmBI sites for inserting sgRNA sequences (Addgene plasmid #62205)<sup>141</sup>.

Candidate sgRNA were identified by the following publicly available tool:

<https://portals.broadinstitute.org/gpp/public/analysis-tools/sgrna-design-crisprai>. We identified high-scoring candidate sgRNA to four target regions within and flanking the *Soat1* transcriptional start site (TSS). To examine potential off-target matches, we used BLAST for each sequence against both the human and HHV-5 (another name for HCMV) genomic database (<https://blast.ncbi.nlm.nih.gov>). The sequences used to develop sgRNA targets are listed under **Table 3**.

**Table 3. sgRNA sequences used for developing CRISPR-knockout or CRISPRi-knockdown cells.**

sgRNA Primer Set	Primer 1	Primer 2
Non-Targeting (NT) – CRISPR	CACCGCGCTTCCGCG GCCCGTTCAA	AAACTTGAACGGGCC GCGGAAGCGC
Non-Targeting (NT) – CRISPRi	ACACCGCGCTTCCGCG GGCCCGTTCAAG	AAAACCTTGAACGGGC CGCGGAAGCGCG
PERK Set 1	CACCGTGGAGCGCGC CATCAGCCCCG	AAACCGGGCTGATGG CGCGCTCCAC
SOAT1 Set 1	ACACCGGCCAGCAGG AAGGTCGACTCG	AAAACGAGTCGACCT TCCTGCTGGCCG
SOAT1 Set 2	ACACCGTGGGCGCCA GGAGAGCTTCCG	AAAACGGAAGCTCTC CTGGCGCCACG
SOAT1 Set 3	ACACCGCGCCTGCTA AGCTAAAGCGCG	AAAACGCGTTTAGCTTA GCAGGCGCG
SOAT1 Set 4	ACACCGTGGCCCTGC GCGTGACGCAGG	AAAACCTGCGTCACG CGCAGGGCCACG

## 2.7. Lentivirus Production

Either the lentiCRISPR v2, pHAGE TRE dCas9-KRAB, or pLenti SpBsmBI sgRNA Hygro plasmid constructs were co-transfected with a lentiviral packaging plasmid (psPAX.2) and envelope plasmid (pMD.2G) into 293FT cells using the X-tremeGENE 9 DNA transfection reagent (Roche), according to the manufacturer's protocol. lentiCRISPR v2 pseudo-lentivirus was collected at 72 h post-transfection and

treated onto life-extended HFF (HFF-hTERT) cells. Supernatant containing dCas9-KRAB pseudo-lentivirus was collected at 72 h post-transfection, supplemented with 8 $\mu$ g/mL polybrene, and treated onto primary HFF cells. Supernatant containing all four SOAT1 sgRNA pseudo-lentivirus was similarly collected and used on HFF-dCas9 cells.

## Chapter 3: Results

### 3.1. HCMV induces CE biosynthesis

#### Introduction

HCMV replication requires remodeling numerous metabolic pathways. HCMV up-regulates metabolic flux through multiple metabolic pathways, particularly those that control the flow of glucose-derived carbons to lipids<sup>49,50,53</sup>. Our lab is specifically interested in understanding the role of lipid metabolism in HCMV replication. To understand how HCMV manipulates host lipid metabolism, we identified global lipid changes that occur once cells are infected with HCMV.

#### Results

Since HCMV induces elongation of very long-chain fatty acids (VLCFAs), the Purdy lab performed an untargeted lipidomic screen using LC-MS/MS to identify lipids with VLCFA tails. Among various lipids altered by HCMV, CE levels were strongly enhanced. CEs are neutral lipids but must have a charge to be detected by mass spectrometry. Electrospray ionization produces charged adducts (such as  $[M + \text{NH}_4]^+$  or  $[M + \text{Na}]^+$ ) of CE (**Figure 3A**)<sup>134</sup>. To develop our LC-MS/MS analysis of CE lipids, we compared the abundance of CE species with both the  $\text{NH}_4$  or Na adducts and found that CE abundance was slightly skewed towards the  $\text{NH}_4$  adduct (**Figure 3B**). Given this observation, to quantitatively define how infection alters CEs we calculated the fold-change in CE+adduct species between mock- and HCMV-infected cells ( $\Delta\text{CE}$ ) for each adduct. For the final value reported here, we averaged the  $\Delta\text{CE}$  for CE+ $\text{NH}_4$  adduct and

the  $\Delta CE$  for the CE+Na adduct if both forms were measured. Results were calculated from the following equation:

$$\Delta CE(18:1) = \frac{[(\Delta CE(18:1) + NH_4)^+ + (\Delta CE(18:1) + Na)^+]}{2}$$

In this example, we define  $(\Delta CE(18:1)+NH_4)^+$  as the fold-change in CE(18:1) identified with the  $NH_4$  adduct,  $(\Delta CE(18:1)+Na)^+$  as the fold-change in lipids identified with the Na adduct, and  $\Delta CE(18:1)$  as an average between the  $NH_4$  and Na values.

Since our observations may be affected by lipids in fetal bovine serum (FBS), we measured CE lipids in our FBS using LC-MS/MS. We found that FBS contains multiple CE lipid species (**Figure 4**). To limit their effect on our experiments, we removed the serum from our cells 1 day before we initiated the experiment by infecting the cells.

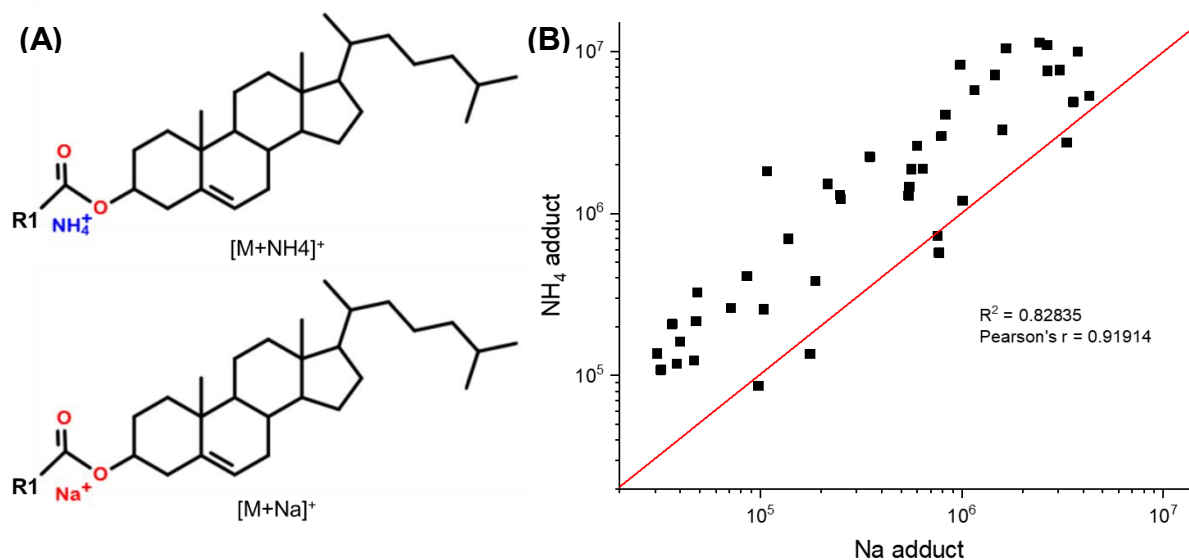


**Figure 3. LC-MS/MS analysis of CE lipid detection between  $NH_4$  and Na adducts.**

(A) Detection of CE lipids with LC-MS using  $NH_4^+$  and  $Na^+$  adducts. (B) Linear regression plot between relative amounts of CE species detected with the  $NH_4$  and Na adduct. The red line indicates what a perfect linear fit would look like.

To test if HCMV alters CE levels, we infected cells for 1h with 3 infectious HCMV units per cell (multiplicity of infection, MOI = 3). Uninfected – i.e. mock-infected – cells were treated the same but lacked the addition of HCMV. Lipids were extracted from uninfected and HCMV-infected cells every 24h over 3d. This time course covers the entire viral replication process from immediate-early to late. CEs were quantitatively measured by LC-MS/MS analysis. CEs were identified by LC retention time and the  $m/z$  value of the precursor ion. Lipids were confirmed by identifying the conserved headgroup after fragmentation using high-energy collisional dissociation MS/MS. HCMV-infected cells contained higher CE levels compared to uninfected cells (**Figure 5**). CEs increased by 24 hpi and remained elevated throughout viral infection (**Figure 5A-B**). However, the greatest levels of CE were observed at 24 hpi. Since we began serum starvation 24 h prior to infection and cells were maintained in serum-free medium for the duration of the experiment, we performed one experiment to test the effect of serum starvation of CEs in uninfected cells. We found that uninfected cells that are

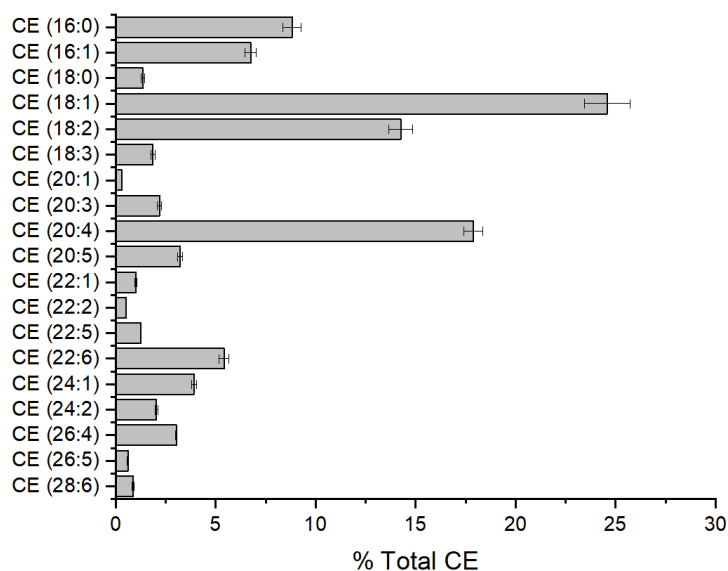


#### Figure 4. CE are present in FBS.

Total lipids from FBS was extracted and analyzed by LC-MS/MS. Data is represented as percent composition of total CE species detected.

All data are represented as mean  $\pm$  SEM of at least three independent experiments.



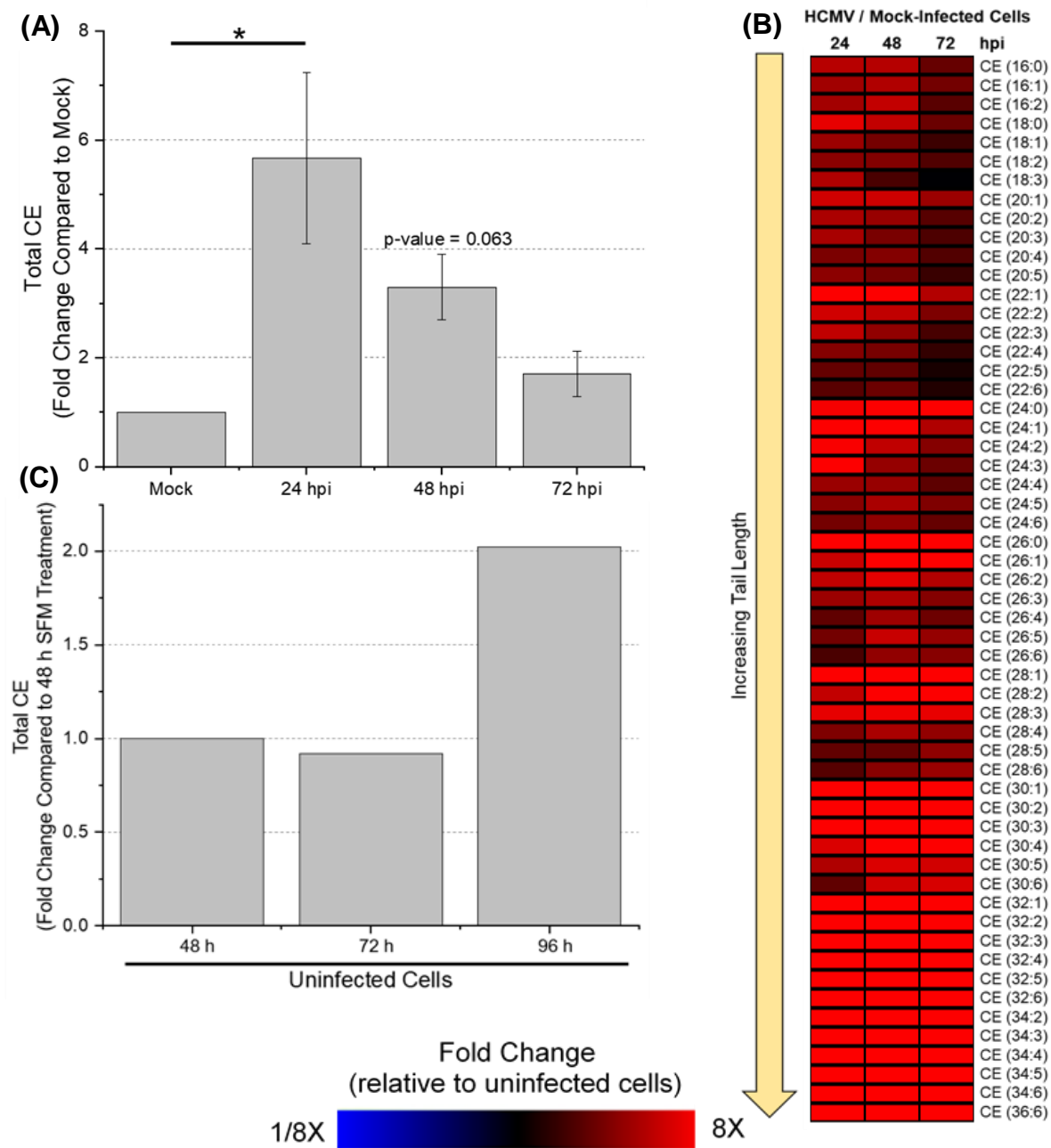


**Figure 5. HCMV-infected cells contain greater levels of CE lipids in fibroblast cells.**

HFF cells were infected with AD169 (3 IU/cell) in serum-free medium. Total lipids from cells were extracted at the designated timepoint and analyzed by LC-MS/MS. **(A)** Fold-change in total CE signals were compared to mock-infected cells. **(B)** Heatmap colors representing a 1/8 to 8-fold scale compared to mock-infected cells. **(C)** Fold-changed in total CE signals in uninfected cells were compared to 48 h SFM treatment.

Data from 5A-B are represented as mean  $\pm$  SEM of at least three independent experiments. Significance was determined by students t-test: \* $p \leq 0.05$ .

serum-starved for 96 h have 2-fold greater levels of CE when compared to 48 h serum-starvation (**Figure 5C**). This result suggest that serum starvation also stimulates CE synthesis and that reduction in CE levels at later time points of infection are likely due to an increase in CE synthesis in our uninfected-control cells responding to serum starvation. Further, it is possible that increased CE accumulation in uninfected cells could be an effect of cell confluency. Since HFF cells undergo contact-induced growth inhibition, high levels of confluency will reduce their growth rate and likely decrease their membrane and energy needs. If this results in an excess energy state then energy can be stored as lipids, specifically CEs and triglycerides in lipid droplets. We will need to repeat this experiment to confirm these findings.

Next, we wanted to define how infection alters individual CE species. First, we identified and measured CEs in uninfected HFF cells. The most abundant species was cholesteryl oleate (C18:1) (**Figure 6**). CE species with  $\geq 24$  carbon tails are less abundant, with most individual lipid species only contributing less than 0.3% of total CEs. Although some saturated shorter chains were not measured – i.e. C20:0 and C22:0 – we did observe that C24:0 was also low in uninfected cells. When we further examined HCMV-mediated induction of CE accumulation, we identified all CE species were significantly greater in infected cells (**Figure 5B and 7**). The greatest changes were seen in CE species with  $\geq 30$  carbon and/or monounsaturated fatty acid tails (**Figure 7**). Since our heatmaps are on a 1/8 to 8-fold scale, this can mask the magnitude of change between uninfected and HCMV-infected cells (**Figure 5B**). Therefore, we graphed the fold-change in CE lipids at 24 hpi to demonstrate that, while all CE lipids are elevated in infected cells, the VLCFA-CE species with  $\geq 30$  carbon tails

are 50-254 times greater (**Figure 7**). Since the greatest HCMV-mediated CE induction is seen in the less- abundant VLCFA-CE species, this is consistent with previous observations that HCMV preferentially increases fatty acid elongation<sup>54</sup>.

We next examined how HCMV induces high CE accumulation. Cells can either import extracellular CE, make them via *de novo* biosynthesis, or reduce CE hydrolysis. Since we identified high CE accumulation in infected cells in the absence of serum, this

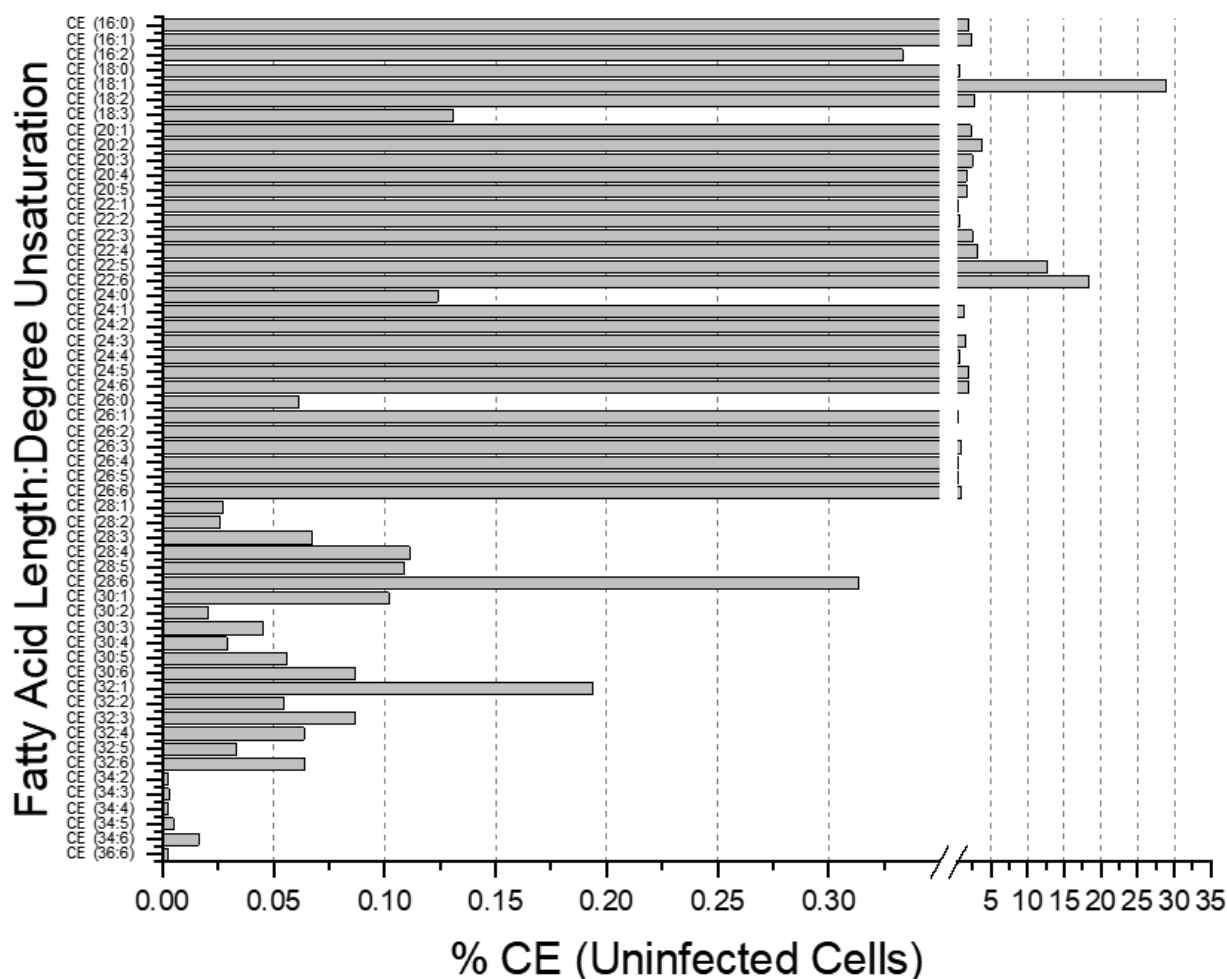


**Figure 6. Characterizing CE population in uninfected HFF cells.**

Confluent HFF cells were maintained in serum-free medium for four days. Total lipids from cells were extracted and analyzed by LC-MS/MS. X-axis breaks are between 0.35 to 0.5.

All data are represented as a mean of at least three independent experiments.

suggests that *de novo* biosynthesis is partially responsible for high CE accumulation. Therefore, we hypothesized that HCMV induces high CE levels by promoting *de novo* biosynthesis. CEs are synthesized by SOAT1 and SOAT2 enzymes (**Figure 8A**). To determine whether SOAT1 and/or SOAT2 gene expression is affected by HCMV replication, we examined their transcriptional levels throughout infection. SOAT1 gene

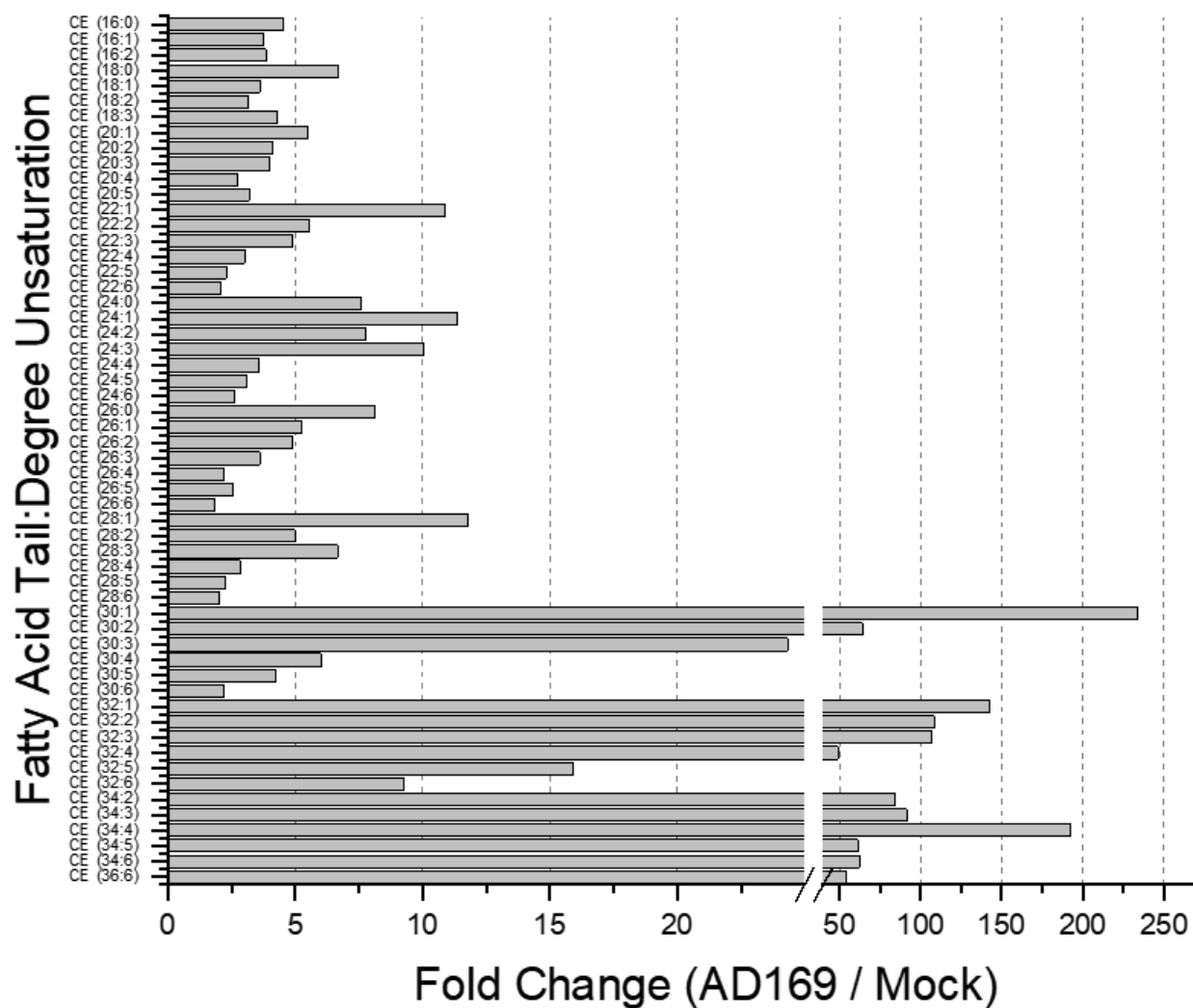


**Figure 7. HCMV-infected cells contain greater CE lipids with LCFA- or VLCFA-tails.**

HFF cells were infected with AD169 (3 IU/cell) in serum-free medium. Total lipids from cells were extracted at 24 hpi and analyzed by LC-MS/MS.

All data are represented as a mean of at least three independent experiments.

expression increases by 24 hpi and progressively increases for the duration of infection, reaching a 5-fold greater expression in infected cells compared to uninfected cells (**Figure 8B**). We concluded that SOAT2 expression was undetectable in both uninfected and HCMV-infected cells after using three different primers. Overall, our data suggest that SOAT1 activity is induced by HCMV.

## Discussion and Future Direction

We found that HCMV promotes high CE levels by 24 hpi. While we identified that global levels of CE are greater in infected cells compared to uninfected cells, there are limitations to our interpretation. Given that our study used LC-MS/MS to capture a 'snapshot' of the lipid profile in infected versus uninfected cells at defined timepoints, we cannot distinguish whether high accumulation of CE is a result of enhanced

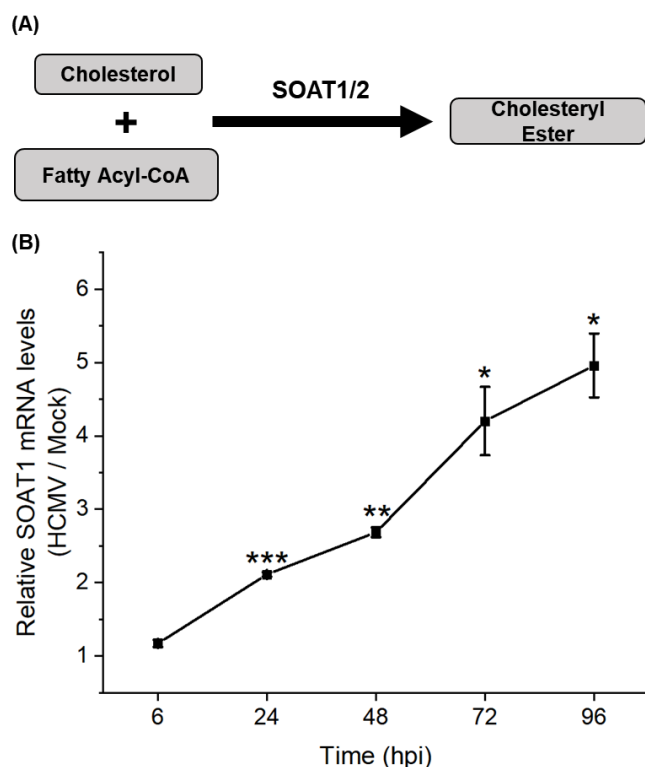


### Figure 8. HCMV induces high CE accumulation through enhanced SOAT1 gene expression.

(A) Diagram of *de novo* cholesteryl ester biosynthesis. (B) SOAT1 mRNA levels throughout the course of HCMV replication. HFF cells infected with AD169 (3 IU/cell) were compared to mock-infected cells for SOAT1 transcripts by qRT-PCR. H6PD was used as the reference gene.

All data are represented as mean  $\pm$  SEM of at least three independent experiments. Significance was determined by the student t test:

\*  $p \leq 0.05$ ; \*\*  $p \leq 0.01$ ; \*\*\*  $p \leq 0.001$ .

biosynthesis or reduced degradation. However, we reason that high CE levels are likely due to enhanced biosynthesis because HCMV induces SOAT1 gene expression and CEs that are not present in the serum-and cannot be imported-are increased by HCMV<sup>53,55</sup>. To more formally define CE synthesis during infection, we would need to perform isotope tracer studies. Cells would be switched from unlabeled media to otherwise identical media containing <sup>13</sup>C-glucose after 1 hpi, leading to labeling of newly synthesized CEs that can be monitored by LC-MS/MS. Since HCMV-infected cells contain high CE levels and SOAT1 gene expression, we predict that HCMV promotes metabolic flux to support high CE biosynthesis.

HCMV promotes the elongation of VLCFAs to support viral maturation and infectivity<sup>53,54</sup>. We detected the greatest induction of unsaturated VLCFA-CE species in HCMV-infected cells compared to uninfected cells. The function of these unsaturated VLCFA-CE species remains undefined. Since CE lipids typically do not incorporate into lipid membranes, we doubt that VLCFA-CE species are required for the viral envelope. Future studies should focus on possible roles from specific CE species during HCMV infection.

HCMV induces lipogenic enzyme expression by 24-48 hpi to support lipid biosynthesis<sup>53-56</sup>. We found HCMV similarly induces SOAT1 gene expression by 24 hpi, which continues to increase for the duration of infection. However, potential mechanisms of virus-mediated SOAT1 induction remains unclear. Unlike most lipogenic enzymes, SOAT1 has not been shown to be regulated by SREBPs; rather, SOAT1 can activate SREBP1 by converting ER-bound cholesterol to CE in glioblastoma<sup>83,102</sup>. Alternatively, HCMV might induce SOAT1 gene expression by upregulating mTOR

activity. SOAT1 gene expression and CE accumulation are regulated by mTOR-mediated activation of PPAR $\gamma$ <sup>69,106,142,143</sup>. HCMV early protein pUL38 supports mTOR-mediated fatty acid elongation by inhibiting the tuberous sclerosis protein complex (TSC1/2), which would otherwise interfere with mTOR activation<sup>54</sup>. However, our lab found that pUL38 expression does not affect CE accumulation (*data not shown*). We will need to directly examine whether HCMV-mediated mTOR activation affects CE accumulation.

Since CE levels are increased by 24 hpi, we hypothesize that an immediate-early or early factor may be important for HCMV-induced CE synthesis. One immediate early protein is pUL37 exon 1 (pUL37x1), which has been predicted to be important for metabolism<sup>144</sup>. pUL37x1 is a viral mitochondrial inhibitor of apoptosis that promotes Ca<sup>2+</sup> release from the ER into the cytosol<sup>127</sup>. It is possible that pUL37x1-mediated Ca<sup>2+</sup> release activates CaMKK, thus leading to AMP-activated protein kinase (AMPK) activation<sup>47,127</sup>. AMPK activation typically suppresses fatty acid and cholesterol biosynthesis by phosphorylating both ACC1 and HMGCR. However, HCMV virion production requires sufficient fatty acid and cholesterol biosynthesis so the virus interferes with AMPK-mediated enzymatic inhibition<sup>47,52,145</sup>. Therefore, we hypothesize that HCMV pUL37x1 induces high CE accumulation. In addition to promoting CaMKK-mediated AMPK activation, ER Ca<sup>2+</sup> homeostasis regulates the activity of the ER stress sensor PKR-like endoplasmic reticulum kinase (PERK)<sup>62</sup>. Given that HCMV induces PERK for lipid biosynthesis, we will examine whether PERK activation modulates CE accumulation<sup>61</sup>.

## 3.2 Viral mechanisms of induced CE biosynthesis

### Introduction

pUL37x1 is a viral mitochondrial inhibitor of apoptosis that also promotes  $\text{Ca}^{2+}$  release from the ER into the cytosol to reorganize the actin cytoskeleton<sup>127</sup>. ER  $\text{Ca}^{2+}$  homeostasis regulates the activity of the ER stress sensor PKR-like endoplasmic reticulum kinase (PERK), which promotes the expression of lipogenic enzymes during HCMV replication<sup>62,61</sup>. Given that pUL37x1 promotes  $\text{Ca}^{2+}$  release from the ER and HCMV induces PERK for lipid biosynthesis, we examined whether pUL37x1 expression and PERK activation modulates CE accumulation.

### Results

Given that pUL37x1 expression induces  $\text{Ca}^{2+}$  release that regulates lipid biosynthesis, we investigated if pUL37x1 is necessary for high CE accumulation. We infected HFF cells with either the AD169 wild-type (AD*wt*) or a mutant AD169 strain that lacks pUL37x1 expression (AD*sub*UL37x1) (**Figure 9A, image kindly provided by Yuecheng Xi**). The AD*sub*UL37x1 mutant virus was generated by allelic exchange, resulting in the deletion of 487bp (lacks the sequence from 169,144 – 169,631bp)<sup>127</sup>. The AD*sub*UL37x1 mutant virus has a severe growth defect, yielding less infectious virions at later timepoints when compared to AD*wt*<sup>127</sup>. At 48 and 72 hpi, we extracted lipids and analyzed CE accumulation by LC-MS/MS. The AD*sub*UL37x1 mutant virus induced slightly higher CE levels compared to uninfected cells (**Figure 9B and 9C, left-side**). However, the AD*sub*UL37x1 mutant virus' ability to induce high CE accumulation



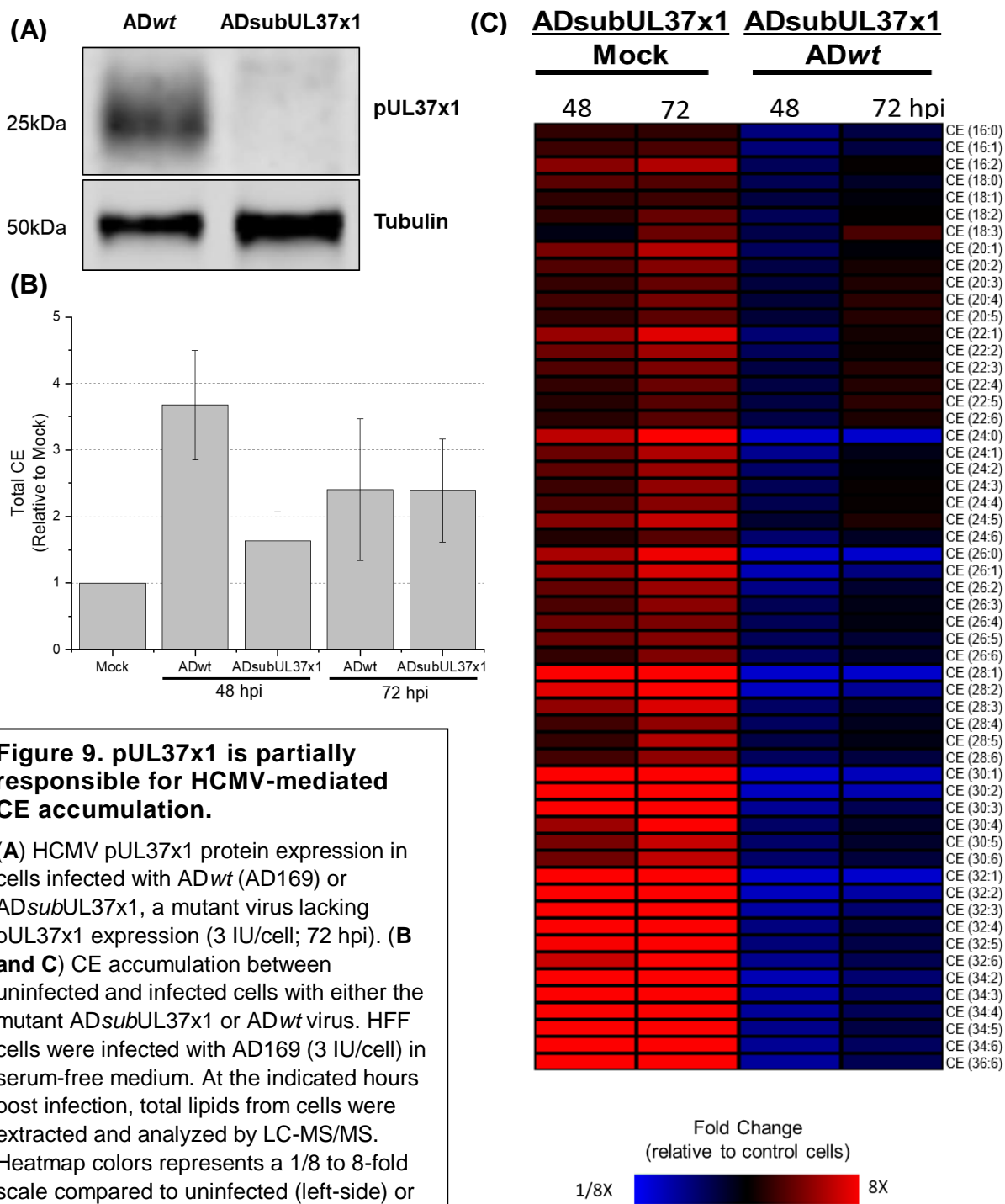


**Figure 9. pUL37x1 is partially responsible for HCMV-mediated CE accumulation.**

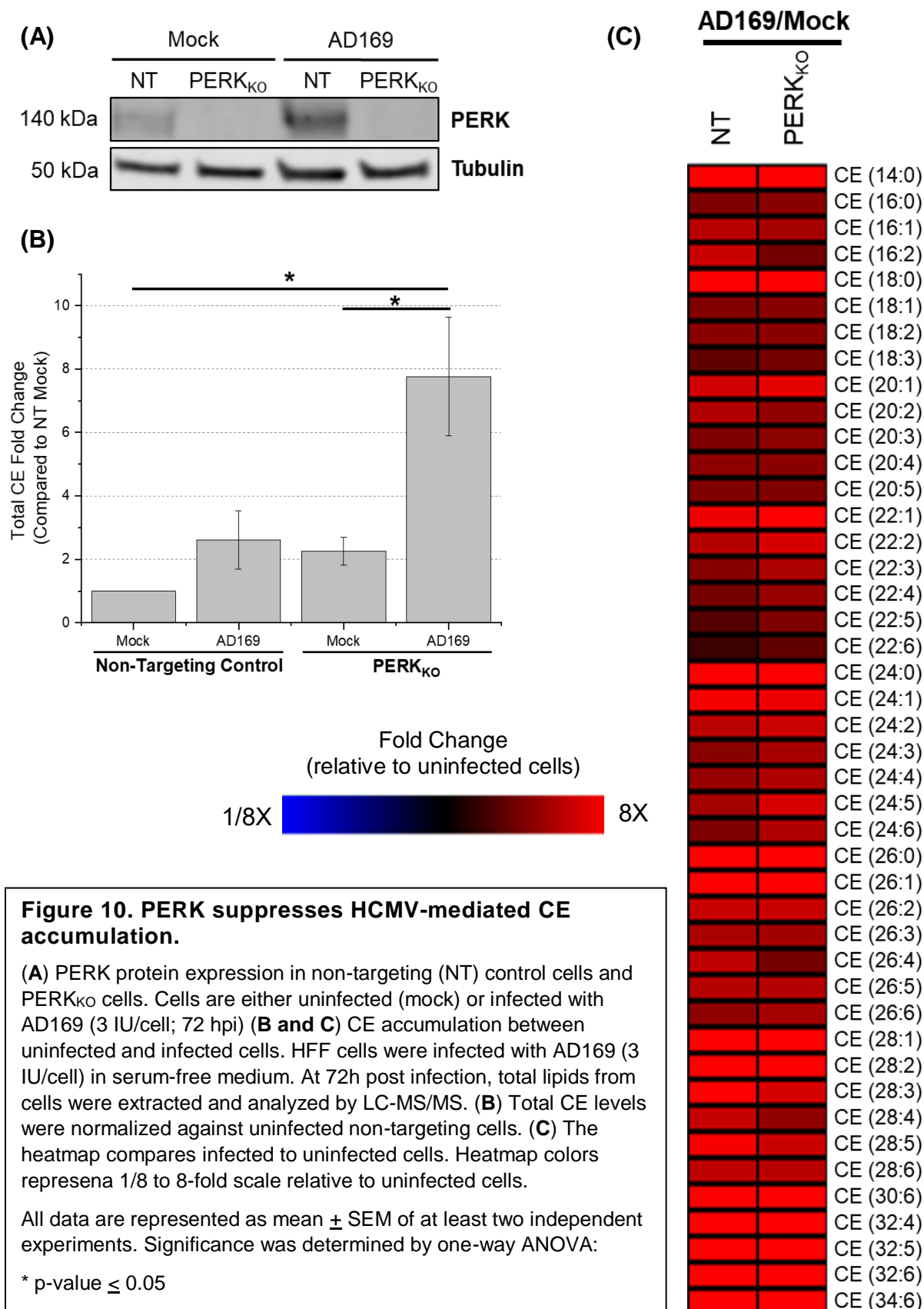
**(A)** HCMV pUL37x1 protein expression in cells infected with *ADwt* (AD169) or *ADsubUL37x1*, a mutant virus lacking pUL37x1 expression (3 IU/cell; 72 hpi). **(B and C)** CE accumulation between uninfected and infected cells with either the mutant *ADsubUL37x1* or *ADwt* virus. HFF cells were infected with AD169 (3 IU/cell) in serum-free medium. At the indicated hours post infection, total lipids from cells were extracted and analyzed by LC-MS/MS. Heatmap colors represents a 1/8 to 8-fold scale compared to uninfected (left-side) or wildtype-infected cells (right-side).

All data are represented as mean  $\pm$  SEM of at least two experiments. Significance was determined by one-way ANOVA.

was slightly deficient at 48 hpi, but not 72 hpi (**Figure 9B and 9C, right-side**). CE species with saturated or mono-unsaturated fatty acid tails were most significantly reduced when pUL37x1 is absent. In addition, cells infected with the *ADsubUL37x1* mutant virus showed reduced CE with VLCFA tails. Our data demonstrates that at least part of HCMV-induced CE levels depend on pUL37x1.

pUL37x1 triggers the release of  $\text{Ca}^{2+}$  stores from the ER into the cytoplasm. A disruption in  $\text{Ca}^{2+}$  homeostasis induces ER stress and activates the unfolded protein response, including PERK<sup>60,62</sup>. Since pUL37x1 is partially responsible for HCMV-mediated CE accumulation, we next examined whether HCMV similarly relies on PERK. CRISPR-mediated PERK knockout was confirmed by western blot (**Figure 10A, image kindly provided by Yuecheng Xi**) and sequencing (data not shown). To test whether PERK is required for CE accumulation during HCMV replication, we infected PERK knockout (PERK<sub>KO</sub>) and non-targeting (NT) control cells and extracted lipids for LC-MS/MS analysis. PERK knockout induces a 2-fold increase in CE accumulation in the absence of infection (**Figure 10A**). When infected, PERK<sub>KO</sub> cells showed a ~3-fold increase in CE accumulation when compared to infected NT cells (**Figure 10A and 10B**). Additionally, there was an ~8-fold increase in infected PERK<sub>KO</sub> cells compared to uninfected NT cells (**Figure 10A**). These results suggest that PERK suppresses CE accumulation, particularly during HCMV replication.

Overall, these results demonstrate that pUL37x1 is partially responsible for high CE accumulation while PERK suppresses CE accumulation during infection (**Figure 11**).



## Conclusions and future directions

We found that HCMV strongly induces high CE accumulation, in part, by pUL37x1. Although AD<sub>sub</sub>UL37x1-infected cells still contained greater levels of CE compared to uninfected cells, there was a downregulation of VLCFA-CE species compared to AD<sub>wt</sub>-infected cells. These observations argue that HCMV induces CE accumulation through a second addition pathway, independent of pUL37x1. Given that SOAT1 transcriptional levels are elevated by 24 hpi, we predict additional viral protein(s) expressed with immediate-early or early kinetics are responsible for efficient CE accumulation.

It remains unclear whether pUL37x1 induces SOAT1 gene expression. Since pUL37x1 expression does not affect lipogenic enzyme expression, we speculate that pUL37x1 is similarly not critical for HCMV-mediated SOAT1 expression (Purdy Lab unpublished). Rather, pUL37x1 might be important for enzymatic activity. Our lab found that pUL37x1 deficiency reduces fatty acid elongation, suggesting that HCMV relies on pUL37x1 to stimulate lipogenic activity (Purdy Lab unpublished). On the other hand, SOAT1 is not thought to be traditionally regulated like most lipogenic genes (i.e. by

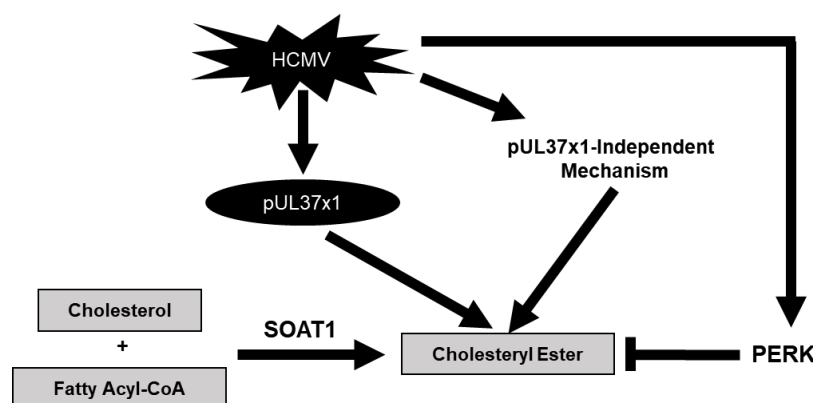


**Figure 11. Diagram of mechanism by which HCMV influences CE accumulation.**

SREBPs), so we will need to confirm whether pUL37x1 induces SOAT1 gene expression<sup>83</sup>.

One of pUL37x1's functions is to release  $\text{Ca}^{2+}$  stores from the ER into the cytoplasm. It is possible that a consequence of pUL37x1 involves disruption of ER  $\text{Ca}^{2+}$  homeostasis and activation of the unfolded protein response. HCMV activates PERK to promote lipid biosynthesis<sup>60,61</sup>. Given that HCMV-induced lipid synthesis requires PERK, we predicted that HCMV relies on PERK to induce CE accumulation. We were initially surprised when we discovered that PERK suppresses CE accumulation in HCMV-infected cells. An explanation to this phenomenon could be due to PERK-mediated activation of autophagy. The PERK/eIF2 $\alpha$  pathway is essential for induction of autophagy as a response to  $\text{Ca}^{2+}$ -mediated ER stress<sup>146</sup>. Autophagy itself regulates lipid metabolism; Singh *et al.* found that loss of autophagy increases lipid droplet accumulation, suggesting that autophagy is important for lipid droplet degradation<sup>147</sup>. Therefore, we initially speculated that HCMV-infected PERK<sub>KO</sub> cells are unable to induce ER stress-mediated autophagy, leading to elevated CE accumulation. However, early viral proteins inhibit autophagy, which is a host defense against infection<sup>148,149</sup>. It would therefore be contradictory for HCMV to activate PERK-mediated autophagy. Future studies focused on the role of autophagy in HCMV-mediated lipid biosynthesis is required.

Overall, our data suggest that HCMV encodes for at least one viral protein that is responsible for high CE accumulation and that PERK regulates CE accumulation. Since HCMV manipulates CE levels early during infection, we next want to test whether we can use CE biosynthesis as an antiviral target against HCMV.

### 3.3. The importance and implications of CE for HCMV replication

#### Introduction

Since HCMV induces SOAT1 gene expression and high CE accumulation by 24 hpi, we hypothesized that CE biosynthesis is important for successful viral replication and that inhibition of SOAT1 will block viral replication. We will test our hypothesis by treating infected cells with avasimibe and TMP-153, both small-molecule inhibitors of SOAT1-2<sup>150-152</sup>. Avasimibe is a synthetic SOAT1-2 inhibitor that was designed with improved bioavailability while TMP-153 is a selective, non-competitive inhibitor<sup>150-152</sup>.

#### Results

Given that the most dramatic changes were observed at earlier timepoints, we hypothesized that CE biosynthesis supports early stages of HCMV replication. We first tested the importance of CE biosynthesis to HCMV replication by treating infected cells with avasimibe. Although avasimibe will inhibit both SOAT1 and SOAT2, we have found that human fibroblast cells only express SOAT1, thus in these experiments we are examining the role of SOAT1 activity during HCMV replication<sup>115,150</sup>. In serum-free conditions, up to 1 $\mu$ M avasimibe was non-cytotoxic while concentrations as low as 2 $\mu$ M induced considerable cell death (**Figure 12A**). Interestingly, we found that fetal bovine serum (FBS) protected uninfected HFF cells from avasimibe-induced cell death. Significant cytotoxic effects were only detected with concentrations greater than 30 $\mu$ M (**Figure 12B**). This may be a similar phenomenon seen by Lee *et al.*, who reported that BSA binds to avasimibe and interferes with SOAT inhibition<sup>153</sup>.

First, we confirmed that avasimibe inhibits SOAT1 activity in HCMV-infected cells by measuring its CE products. As expected, CE levels were reduced in avasimibe-treated cells compared to DMSO treatment (**Figures 13A-B**). HCMV-infected cells treated with avasimibe had a 90% reduction in CE levels when compared to DMSO-treated cells (**Figure 13B**). Next, we determined if the production of infectious viral progeny depends on SOAT1 activity. We added the SOAT inhibitor following a 1 h infection period. Since our goal is to determine if HCMV-induced CE synthesis is important for virus replication, we decided to treat cells after allowing the virus to attach and enter cells. Given that FBS contains CE lipids (**Figure 4**) and potentially interferes with avasimibe (**Figures 12A-B**), we performed viral titer experiments in serum-free medium. At 96 hpi, we measured the number of infectious HCMV virions released by avasimibe and DMSO treated cells. 1 $\mu$ M avasimibe treatment in the absence of serum

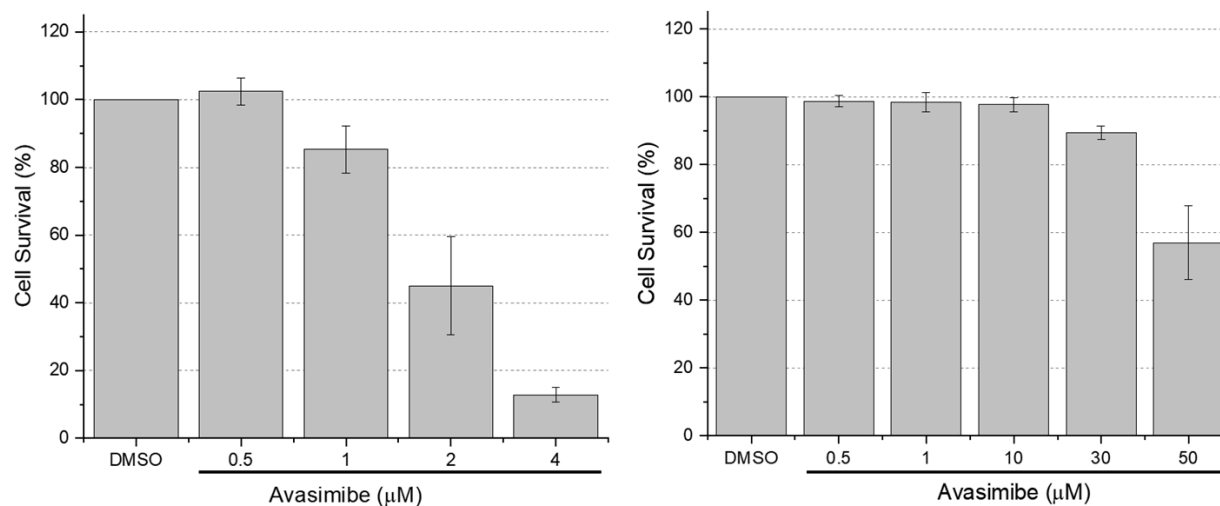
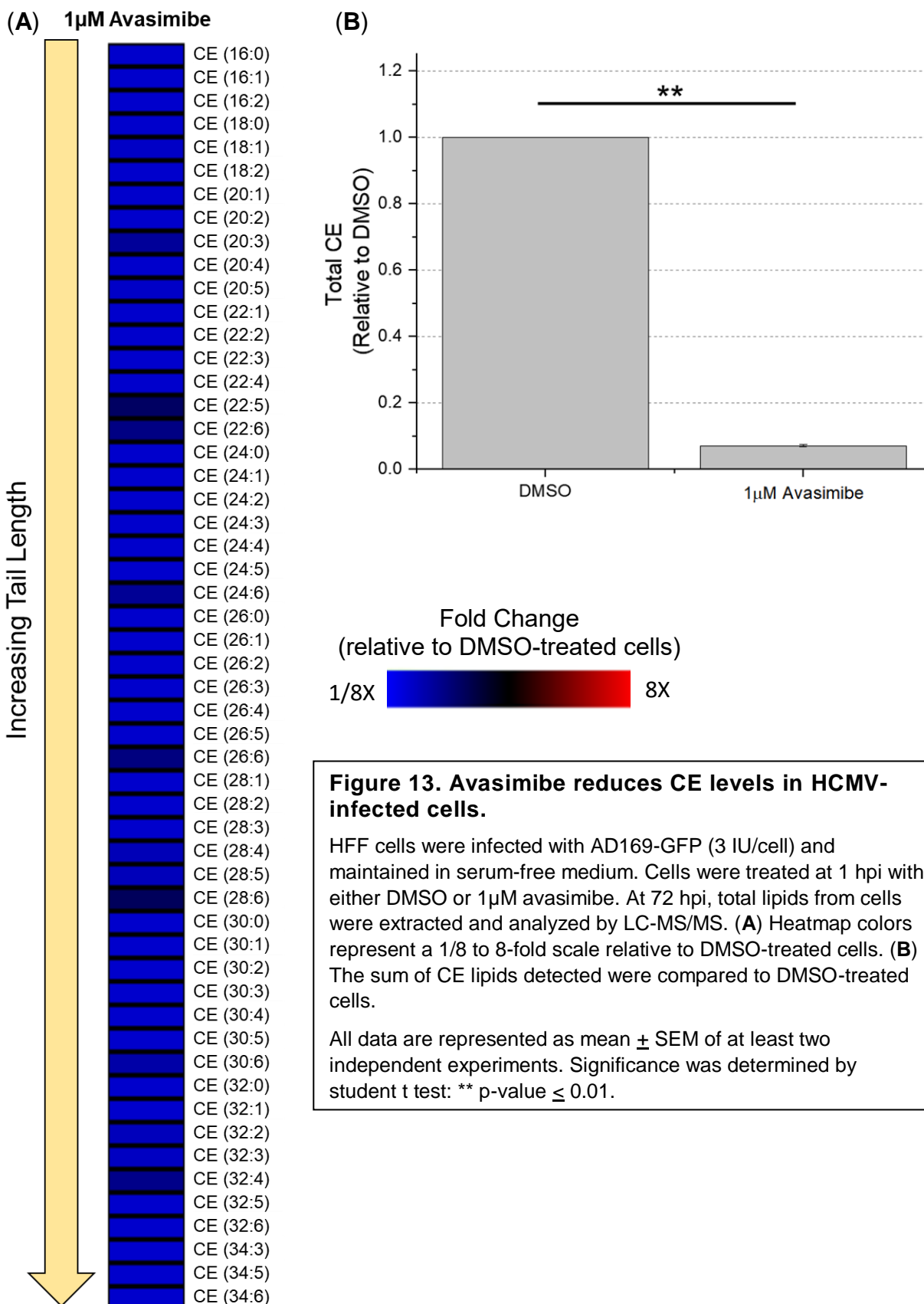


**Figure 12. Avasimibe cytotoxicity in uninfected fibroblast cells.**

Cell viability was measured at 96 h post treatment. Avasimibe treatment under (A) serum-free conditions or (B) supplemented with 10% FBS.

All data are represented as mean  $\pm$  SEM of at least three independent experiments.





completely blocked the production of infectious virions (**Figure 14A**). When infected cells were treated with 1 $\mu$ M avasimibe in the presence of serum, viral replication was rescued (**Figure 14B**). Our observations are like those observed in hepatitis C virus infection (HCV), where avasimibe interferes with its replication. In the case of HCV, blocking SOAT activity limited lipid droplet accumulation which is necessary for infection<sup>116</sup>.

Given that the most dramatic changes were observed at earlier timepoints, we hypothesized that CE biosynthesis supports early stages of HCMV replication. HCMV viral replication is highly organized and occurs in a cascade-like series of events. Immediate early (IE) genes are required for subsequent viral gene expression and overall efficiency of viral replication<sup>34</sup>; early gene expression is necessary for viral DNA replication<sup>35</sup>; and late genes, whose expression is dependent on viral DNA replication,

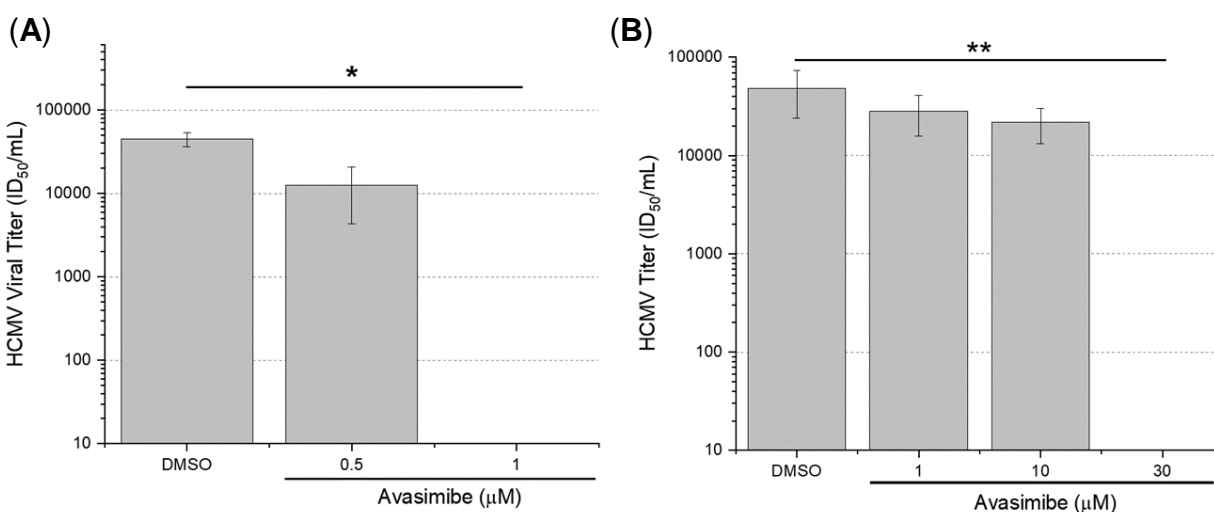


**Figure 14. Avasimibe blocks HCMV viral replication.**

HFF cells were infected with AD169-GFP (3 IU/cell) and treated at 1 hpi with either DMSO or avasimibe. Viral titer was measured at 96 hpi. Cells were either maintained in (A) serum-free medium or (B) medium supplemented with 10% FBS.

All data are represented as mean  $\pm$  SEM of at least two independent experiments. Significance was determined by one-way ANOVA: \* p-value  $\leq$  0.05; \*\* p-value  $\leq$  0.01.

encodes for viral proteins required for virion maturation<sup>36</sup>. We examined avasimibe's impact on viral replication by examining the expression of HCMV's IE protein pUL123, early protein pUL26, and late/tegument proteins pUL82 and pUL99. Treating HCMV-infected cells with 1 $\mu$ M avasimibe blocks pUL26 expression throughout viral replication (**Figure 15**). While we did detect late proteins pUL82 and pUL99 in the presence of avasimibe, their expression remained unchanged throughout the majority of viral replication. Since these viral proteins are also present within the virion tegument, it is likely that the late proteins detected were released upon viral entry instead of late viral gene expression. We confirmed avasimibe's impact on early stages of viral replication by measuring viral DNA accumulation. Since early viral protein expression is required to

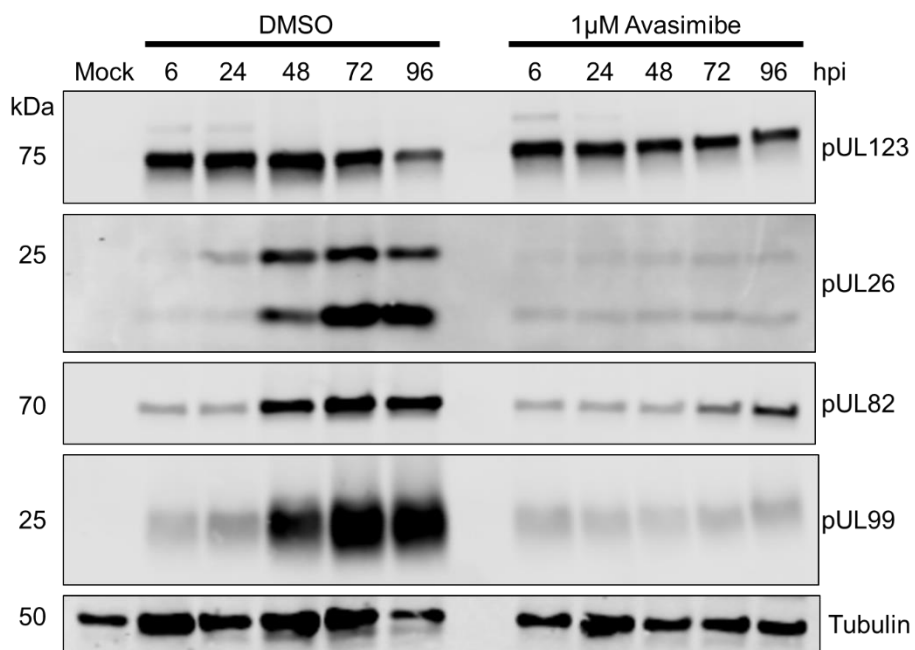


**Figure 15. Avasimibe treatment interferes with HCMV early protein expression.**

HFF cells were infected with AD169-GFP (3 IU/cell) and maintained in serum-free medium. Cells were treated at 1 hpi with DMSO or 1 $\mu$ M avasimibe. Whole cell lysate was collected at the indicated hours post infection and analyzed by western blot. Tubulin was used as the loading control.

Figure is a representative of two independent experiments.

induce viral DNA synthesis, we hypothesized that avasimibe treatment would block viral genome replication. Indeed, infected HFF cells maintained in 10% FBS had significantly reduced viral DNA within 24 h of treating with 30 $\mu$ M avasimibe (**Figure 16**). Despite using two different conditions (10% FBS versus serum-free), avasimibe blocks early stages of HCMV replication. Finally, we confirmed that avasimibe targets early stages of viral replication by treating cells at either 1, 24, 48, or 72 hpi. Infected cells treated at or prior to 48 hpi were unable to produce infectious virions (**Figure 17**). Since early protein expression occurs by 48 hpi, this suggests avasimibe might interfere with both early and late stages of viral replication. While this data further supports the impact of avasimibe

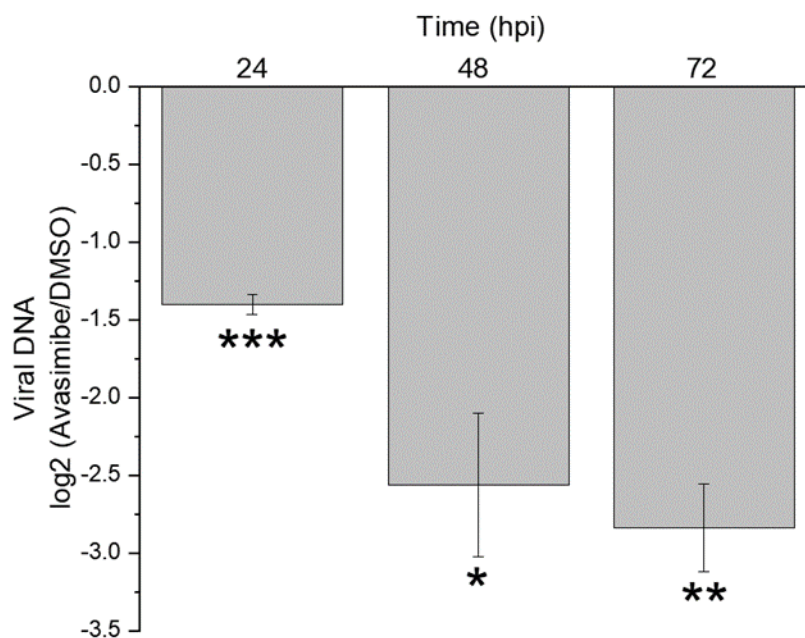


**Figure 16. Avasimibe treatment reduces HCMV viral DNA synthesis.**

HFF cells were infected with AD169-GFP (3 IU/cell) and maintained in growth medium supplemented with 10% FBS. Cells were treated at 1 hpi with DMSO or 30 $\mu$ M avasimibe. Total DNA was collected at the indicated hours post infection and analyzed by qPCR. Viral genomes were measured by using primers for HCMV UL123. Actin was used to measure cellular DNA as a reference.

All data are represented as mean  $\pm$  SEM of at least three independent experiments. Significance was determined by students t test: \* p-value  $\leq$  0.05; \*\* p-value  $\leq$  0.01; \*\*\* p-value  $\leq$  0.001

on HCMV replication, this single experiment needs to be repeated to further define the mechanism behind avasimibe's antiviral effects.

We next examined another SOAT inhibitor, TMP-153, to confirm the significance of CE synthesis towards HCMV replication. In serum-free conditions, up to 400nM TMP-153 was non-cytotoxic (**Figure 18A**). Like avasimibe, fetal bovine serum protected uninfected HFF cells from TMP-153-mediated cell death (**Figure 18B**). We validated TMP-153 inhibits SOAT1 activity in HCMV-infected cells by measuring CE levels. Like we anticipated, 300nM TMP-153-treated cells had a ~85% reduction in CE levels when compared to DMSO treatment (**Figures 19A-B**). We next tested whether TMP-153-mediated SOAT1 inhibition similarly reduced the production of infectious viral progeny by treating cells 1 h post infection. Regardless of whether serum was present, TMP-153

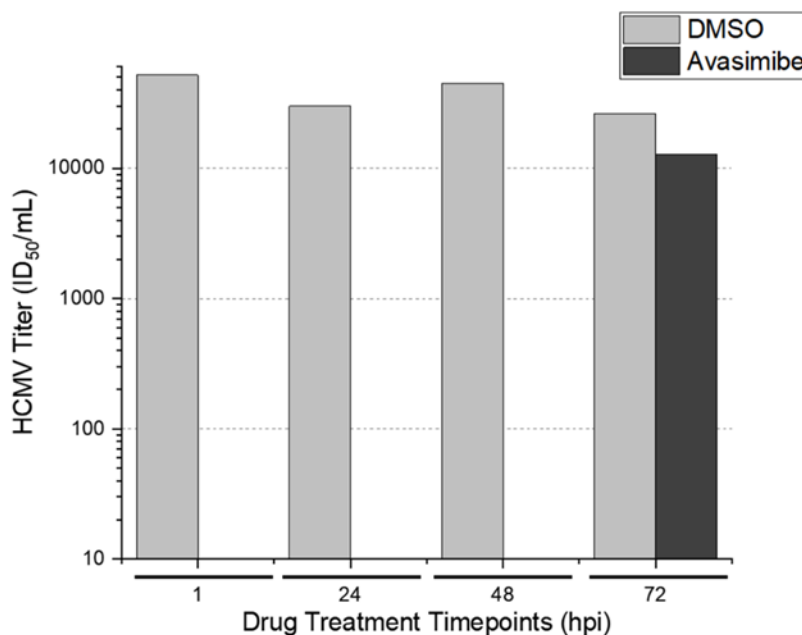


**Figure 17. Avasimibe remains antiviral after treating HCMV-infected cells later during infection.**

HFFs were infected with HCMV (3 IU/cell) in serum-free medium. Cells were treated with DMSO or 1 $\mu$ M avasimibe after 1, 24, 48, or 72 hpi. Viral titer was measured at 96 hpi.

All data is represented as a mean of one experiment.

treatment had no significant impact on HCMV viral titers (**Figures 20A-B**). This observation contradicts what was seen in avasimibe-treated cells, where viral titers were blocked. Since CE levels were similarly reduced between avasimibe-treated and TMP-153-treated cells, this suggests that CE lipids themselves are not important for HCMV replication and that avasimibe's antiviral effects are off-target (**Figure 21**).

## Conclusions and future direction

Since HCMV induces SOAT1 gene expression and high CE accumulation, we wanted to test small-molecule inhibitors against SOAT1 to identify compounds with antiviral activity. We found that non-cytotoxic concentrations of avasimibe suppresses SOAT1 activity and blocks the production of infectious virions. However, avasimibe's

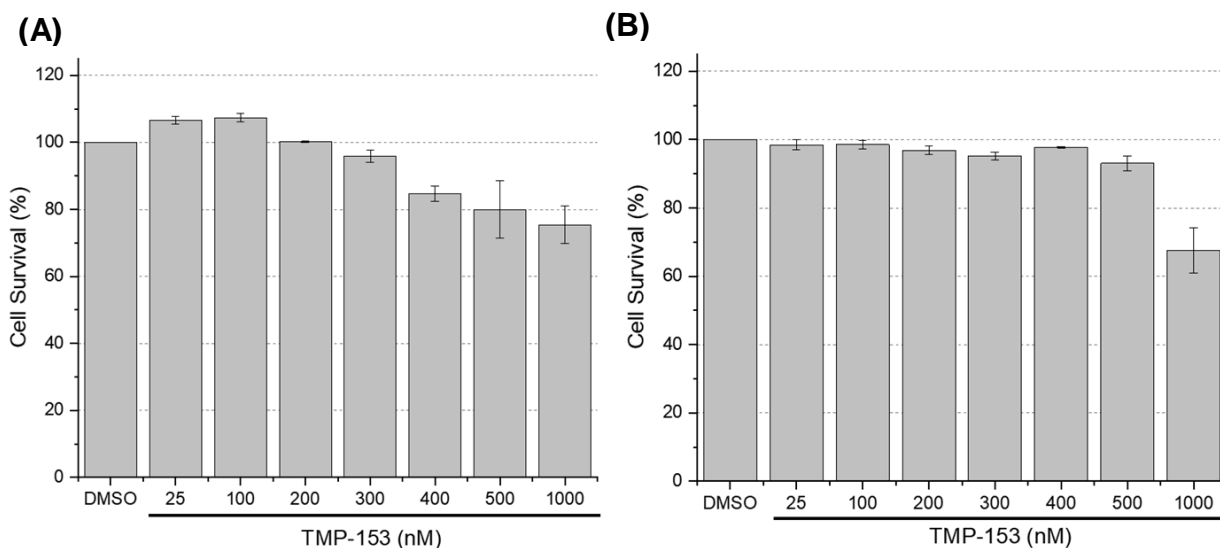
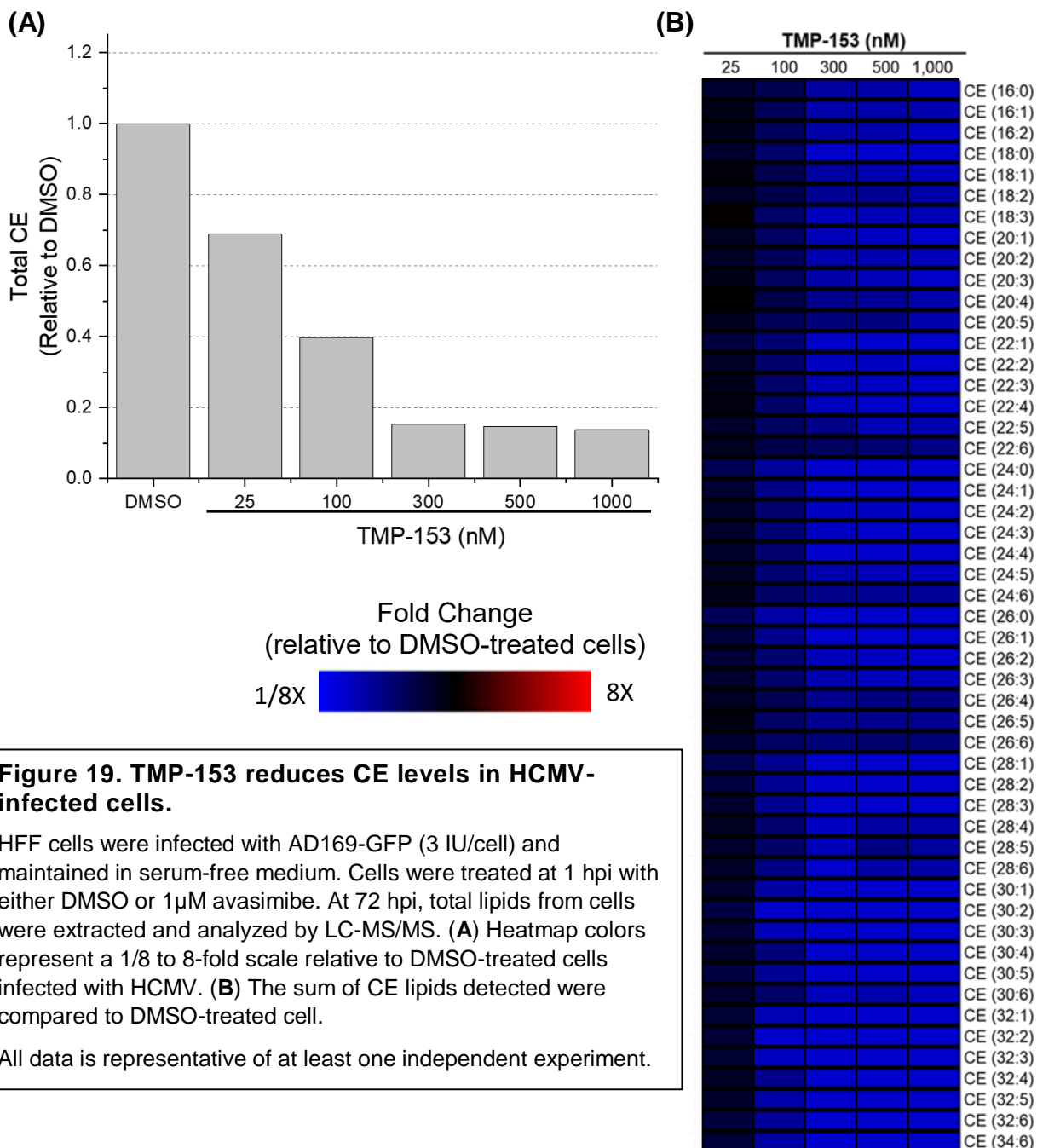


### Figure 18. TMP-153 cytotoxicity in uninfected fibroblast cells.

Cell viability was measured at 96 h post treatment. TMP-153 treatment under **(A)** serum-free conditions or **(B)** supplemented with 10% FBS.

All data are represented as mean  $\pm$  SEM of at least three independent experiments.

cytopathic and antiviral effects were suppressed when cells were supplemented with 10% FBS. One study found that bovine serum albumin binds to avasimibe, preventing it from suppressing SOAT1 activity<sup>153</sup>. Perhaps a similar mechanism of avasimibe interference is seen when cells are provided FBS. Another possibility of cellular protection against avasimibe is the presence of CE in FBS (**Figure 4**). Since infection



induces SOAT1 gene expression and avasimibe suppresses SOAT1 activity, perhaps cells respond to reduced CE levels by importing exogenous CE. However, this second option would suggest that CE lipids are necessary for viral replication. We found that TMP-153 suppresses CE accumulation yet has no effect on viral replication, regardless of whether cells were supplemented with 10% FBS. This suggests that CE lipids themselves are not necessary for HCMV replication. Therefore, it is more likely that the FBS itself is interfering with avasimibe.

Avasimibe blocked viral replication by suppressing early pUL26 expression. Early viral protein expression is necessary for viral genome synthesis<sup>35</sup>. To confirm the effects of avasimibe on early viral protein expression, we will need to test additional viral proteins. HCMV pUL44 and pUL38 are two early viral proteins that can be used to corroborate our findings with pUL26 inhibition by avasimibe. Given that viral genome

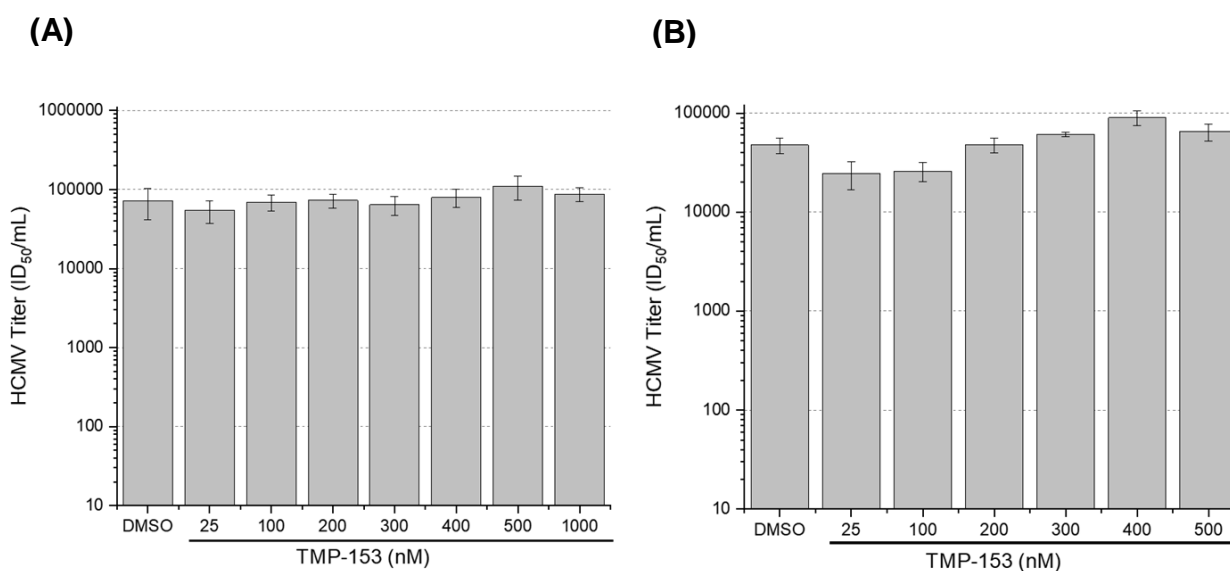


**Figure 20. TMP-153 does not affect HCMV viral replication.**

HFF cells were infected with AD169-GFP (3 IU/cell) and treated at 1 hpi with either DMSO or TMP-153. Viral titer was measured at 96 hpi. Cells were either maintained in (A) serum-free medium or (B) medium supplemented with 10% FBS.

All data are represented as mean  $\pm$  SEM of at least three independent experiments.

synthesis was suppressed by avasimibe, it is likely that avasimibe suppresses early viral protein expression. We will also need to examine the mechanism of avasimibe-mediated interference with early viral protein expression. We can examine whether avasimibe blocks HCMV early gene expression by measuring the transcript levels of early pUL26, pUL44, and pUL38. If there is a suppression of viral gene transcripts, this would suggest that avasimibe blocks viral replication by transcriptionally restraining early gene expression. No differences in gene expression would suggest that avasimibe either blocks early gene translation or promotes viral protein degradation. Further studies are required to define the mechanism of avasimibe antiviral activity against HCMV replication.

We found that 300nM TMP-153 was equally capable of reducing CE levels as 1 $\mu$ M avasimibe, yet TMP-153 treatment did not affect HCMV viral replication. This

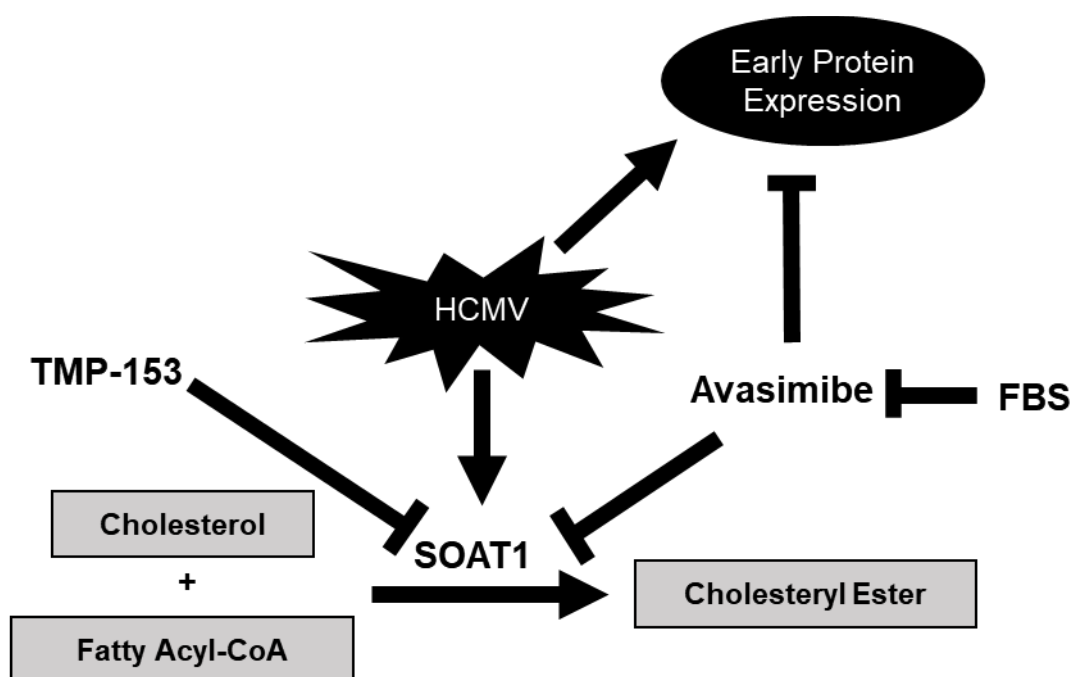


**Figure 21. Diagram of SOAT1 inhibition and avasimibe's mechanism of antiviral activity.**



finding suggests that avasimibe's antiviral effects are independent of SOAT1 activity. Our experiments were performed with a high MOI (3 IU/cell), allowing us to examine a single round of infection. It is possible that we are infecting our cells with a high concentration of virus that allows for enough tegument protein to maintain viral replication when treated with TMP-153. Indeed, we found low levels of late tegument proteins when infected cells were treated with avasimibe (**Figure 15**). We will need to treat cells with SOAT1 inhibitors at a low MOI (0.01 IU/cell) to determine whether SOAT1 activity is important for multiple rounds of infection.

We attempted to directly test the importance of SOAT1 to HCMV replication by developing CRISPR knockout cells. However, we were unable to knockout SOAT1 gene expression due to the Cas9-mediated mutation targeting an intron rather than an exon. Alternatively, we are developing a CRISPR interference (CRISPRi) protocol to knockdown SOAT1 in fibroblast cells. The CRISPRi system uses an RNA-dependent DNA binding protein that lacks endonuclease activity (dCas9), which is recruited by single base-pairing guide RNAs (sgRNAs) to the gene of interest<sup>141</sup>. sgRNA-directed dCas9 recruitment to the transcriptional start site (TSS) downregulates gene transcription by preventing polymerase binding, transcriptional elongation, and transcription factor binding<sup>141,154</sup>. We used qRT-PCR to measure CRISPRi-mediated gene knockdown. Unfortunately, we were only able to knockdown gene expression by  $\leq 50\%$  in uninfected SOAT1-CRISPRi cells (**Figure 22**). We need to further develop our SOAT1-CRISPRi cells to test whether SOAT1 is important for HCMV replication. Likewise, we can use shRNA to knockdown SOAT1 transcripts. Several studies have successfully used shRNA to test SOAT1 implications for diseases, including

glioblastoma and prostate cancer<sup>102,106</sup>. If CRISPRi-mediated SOAT1 knockdown remains insufficient, we can focus on using shRNA as a tool for transcript suppression.

Overall, our results demonstrate that avasimibe blocks early HCMV protein expression and production of infectious virions in a SOAT1-independent mechanism. These results indicate that, while HCMV might not require CE lipids themselves, we can use HCMV as a tool to study SOAT1 and CE metabolism.

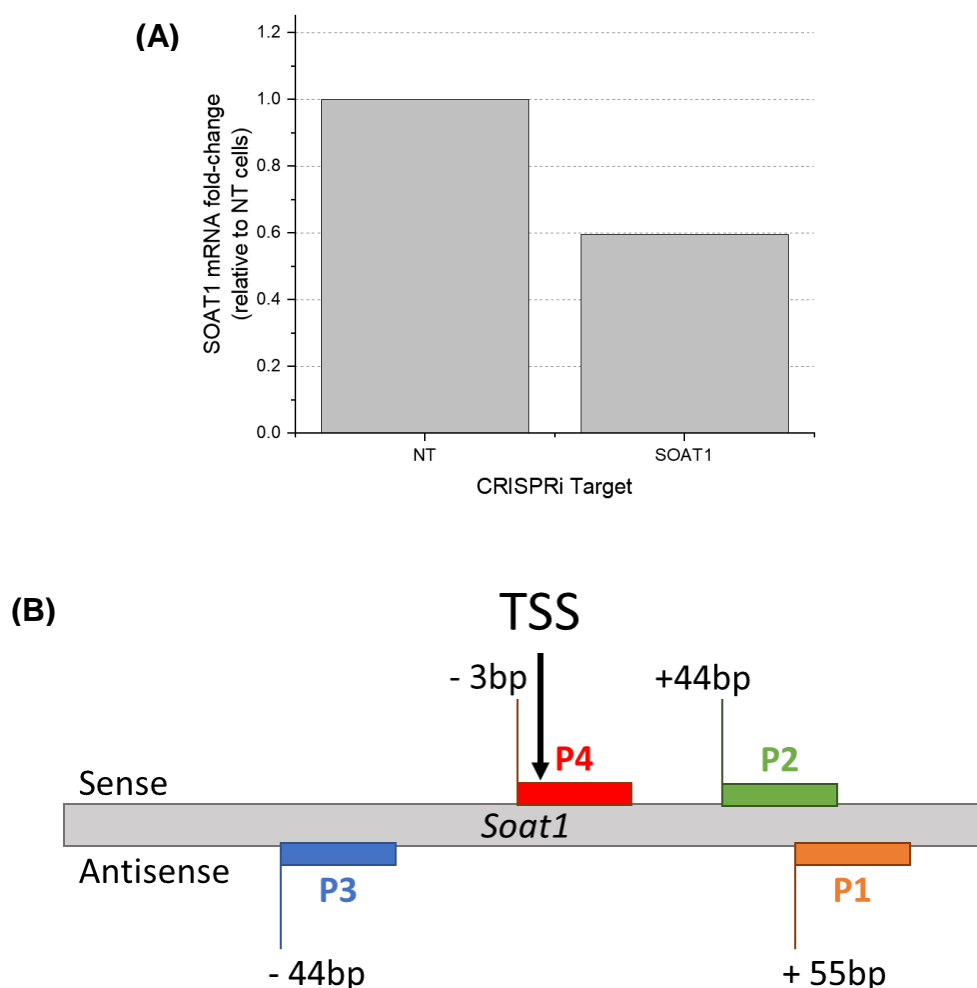


**Figure 22. Design and efficiency of CRISPR-mediated SOAT1 knockdown.**

**(A)** SOAT1 gene expression was only slightly reduced by CRISPRi. Uninfected HFF-dCas9 cells expressing non-targeting (NT) or SOAT1 sgRNA were analyzed by qRT-PCR. H6PD was used as a reference gene. **(B)** SOAT1 sgRNA target design. A publicly-available online tool was used to design sgRNA based on PAM sequence and proximity to the transcription start site (TSS).

## Chapter 4: Discussion

Our lab is specifically interested in understanding the role of lipid metabolism in HCMV infection. Using an untargeted lipidomic screen, we found that CE lipids accumulate in HCMV-infected cells early during infection. Further, HCMV induces SOAT1 gene expression by 24 hpi.

Given that CE are neutral lipids that typically do not associate with lipid membranes, it is unlikely that enhanced CE accumulation is directly associated with viral envelope development<sup>155</sup>. Rather, it is possible that induction of SOAT1 could support a global cellular shift in lipid metabolism during infection. ER-bound sterols suppress activation of the lipogenic transcription factor SREBP1. SOAT1-mediated activation of SREBP1 has been shown to be critical for inducing lipogenic gene expression in glioblastoma and prostate cancer<sup>102,106</sup>. HCMV strongly induces SREBP1 activation by 24hpi and maintained activation for the duration of replication<sup>55</sup>. Since CE accumulation is elevated by 24 hpi, perhaps HCMV uses SOAT1-mediated CE biosynthesis to maintain SREBP1 activation by limiting cholesterol accumulation in the ER. Further examining how SREBP's negative feedback loop is suppressed as virus-mediated lipid biosynthesis is enhanced will provide greater insight into why HCMV induces CE accumulation.

We found that HCMV pUL37x1 protein is partially responsible for CE accumulation during early stages of viral replication. pUL37x1 has two well-established functions: 1) induce Ca<sup>2+</sup> release from the ER and into the cytoplasm and 2) translocate to the mitochondria to block apoptosis<sup>127,156</sup>. Since SOAT1 is localized to the ER, we

predict pUL37x1-mediated  $\text{Ca}^{2+}$  signaling might be responsible for inducing high CE accumulation. One possible mechanism of pUL37x1-mediated CE accumulation involves activation of CaMKK. CaMKK is activated by  $\text{Ca}^{2+}$  release from the ER and is responsible for activating AMPK during HCMV infection<sup>47,130</sup>. Under normal conditions, AMPK activation supports glycolytic flux to support energy production while simultaneously suppressing energy-consuming fatty acid and cholesterol biosynthesis. Inhibition of fatty acid and cholesterol biosynthesis is accomplished by AMPK phosphorylation of ACC1 and HMGCR, which suppresses enzymatic activity. However, HCMV blocks AMPK-mediated lipogenic enzyme inhibition, allowing for AMPK-induced glycolytic flux while maintaining high fatty acid and cholesterol biosynthesis<sup>64</sup>. While it remains unclear how HCMV drives CaMKK activation, we speculate that immediate-early pUL37x1-mediated  $\text{Ca}^{2+}$  release is responsible.

Another possible consequence of immediate-early pUL37x1 disrupting ER  $\text{Ca}^{2+}$  homeostasis could be the activation of PERK as part of the ER stress response<sup>62</sup>. PERK activation attenuates translation while simultaneously promoting lipid biosynthesis<sup>61,62</sup>. Qian *et al.* found that UV-killed MCMV, which are capable of entering a cell but are deficient in viral gene expression, were partially capable of activating eIF2 $\alpha$ /ATF4<sup>157</sup>. They also found that MCMV-infected cells treated with phosphonoacetic acid (PAA), which disrupts viral genome synthesis and blocks late protein expression, still maintained eIF2 $\alpha$ /ATF4 activation<sup>157</sup>. This suggests that both viral entry and immediate early/early gene expression induces PERK activation.

We discovered that PERK suppresses CE accumulation in HCMV-infected cells. Our data suggest that HCMV pUL37x1-mediated CE accumulation is independent of

PERK. Perhaps one possible explanation to PERK-mediated suppression of CE accumulation is autophagy. PERK/eIF2 $\alpha$ /ATF4 activation is necessary for stress-induced autophagy, which reduces lipid droplet accumulation<sup>146,147</sup>. This would suggest that PERK-mediated autophagy regulates CE accumulation during infection. However, there are several observations that contradict this prediction. HCMV regulates autophagy during two phases of infection. McFarlane *et al.* show that HCMV-mediated autophagy is induced by 2 hpi and is independent of viral gene expression, since UV-killed virus were capable of inducing autophagy<sup>158</sup>. At later times during infection, HCMV inhibits autophagy by *de novo* viral protein synthesis<sup>148,149</sup>. Mukhopadhyay *et al.* show that HCMV-mediated activation of mTOR suppresses autophagy<sup>159</sup>. Further, the viral suppression of autophagy was resistant to LiCl, an inducer of autophagy independent of mTOR<sup>148</sup>. This suggests that HCMV has several mechanisms for blocking autophagy during later stages of viral replication. Therefore, it would appear contradictory for HCMV to activate PERK and induce antiviral autophagy. Since we observed greater CE levels in infected PERK<sub>KO</sub> cells; PERK is required for ER stress-induced autophagy; autophagy reduces lipid droplet accumulation; and HCMV suppresses autophagy later during infection, this suggests that PERK regulates CE accumulation independent of autophagy during HCMV infection (**Figure 23**). Further examining how HCMV modifies PERK signaling during infection is required to test PERK-mediated regulation of CE metabolism.

Since HCMV induces high CE accumulation during early stages of replication, we hypothesized that SOAT1 activity can be used as an antiviral target. We first focused on avasimibe, a SOAT1-2 inhibitor that is clinically proven to be safe<sup>160</sup>. While CE lipids

themselves are not critical for HCMV replication, avasimibe shows exceptional antiviral effects when compared to TMP-153. We discovered that avasimibe blocks HCMV pUL26 expression, indicating a potential block in early viral protein expression. HCMV early gene expression is dependent on immediate early protein expression. We found that avasimibe does not affect immediate early pUL123 expression, suggesting that avasimibe interferes with either early viral transcription, translation, or protein stability. Since early viral protein expression is necessary for viral DNA replication, avasimibe-mediated inhibition of early proteins blocked viral genome synthesis. Finally, avasimibe blocked viral replication unless if infected cells were treated after 48 hpi. This observation indicates that avasimibe might similarly interfere with late stages of viral replication. Future studies should focus on determining avasimibe-mediated antiviral mechanism of blocking HCMV protein expression.

Although the specific mechanism for avasimibe-induced HCMV inhibition remains unknown, there are several known off-targets. Avasimibe blocks microsomal triglyceride transfer protein (MTTP) expression, which is required for early stages of VLDL and chylomicron production<sup>116</sup>. One study claims that TMP-153 does not interfere with

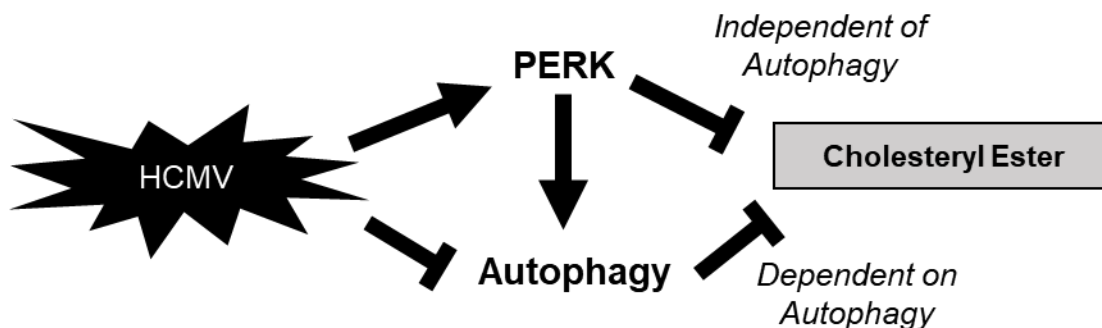


**Figure 23. Possible pathways of PERK-mediated CE regulation during HCMV infection.**

MTTP expression; however, they failed to present data supporting this claim<sup>116</sup>. While it remains untested whether avasimibe's antiviral effects against HCMV results from MTTP interference, several studies have examined triglyceride metabolism in CMV infection. While neither serum chylomicrons nor VLDL were measured, Low *et al.* found that mice infected with MCMV have elevated plasma triglycerides<sup>114</sup>. Like CE lipids, triglycerides are neutral lipids that constitute the core of lipoproteins. Elevated plasma triglycerides might indicate greater lipoprotein secretion during infection. However, the large knockdown screen performed by Koyuncu *et al.* show that HCMV replication increases when the AGPAT9 gene is knocked down<sup>53</sup>. AGPAT9 encodes for the enzyme glycerol-3-phosphate acyltransferase 3 (GPAT-3), which is responsible for the initial steps of triglyceride synthesis<sup>161</sup>. However, the importance of GPAT-3 to HCMV infection was never confirmed. Further, GPAT-3 is important for phospholipid biosynthesis, which our lab has confirmed to be important for HCMV infection (Purdy lab unpublished)<sup>161</sup>. Further research into HCMV, triglyceride metabolism, and lipoprotein secretion is required.

Since small-molecule inhibitors may have off-target effects, we attempted to directly test the importance of SOAT1 to HCMV replication by genetically knocking down SOAT1. However, we only suppressed SOAT1 gene expression by ~40% in uninfected CRISPRi cells. There are several possible explanations why our CRISPRi system failed. Similar to Cas9, chromatin structure and dynamics can influence the success of dCas9 binding<sup>162</sup>. However, trimethylated histone H3 lysine 4 (H3K4me3) was identified as part of the regulation of *Soat1* gene expression in mouse embryonic stem cells, neural progenitor cells, and embryonic fibroblasts<sup>163</sup>. Given that H3K4me3

modifications are typically associated with transcriptional activation, it is unlikely that chromatin structure is blocking dCas9 binding to the *Soat1* TSS. However, further investigation into the epigenetic modification of *Soat1* in human cells is required.

Another possibility on why our SOAT1-CRISPRi system was unsuccessful could be due to our development methodology. The efficiency of individual sgRNA targets is dependent on its proximity to the TSS; targets that are approximately 60bp away from the TSS are less likely to induce significant gene downregulation when compared to targets within 35bp<sup>164</sup>. Depending on the relative positions of the sgRNA, it is possible to increase gene silencing efficiency<sup>164</sup>. We treated our primary HFF-dCas9 cells with a mixture of four lentiviruses expressing different SOAT1 sgRNA targets. We designed our sgRNA targets based on the presence of the PAM sequence and proximity to the *Soat1* TSS (**Figure 22B**). While we were able to hygro-select for HFF-dCas9 cells that were successfully transfected with at least one sgRNA target, we could not screen for cells that contained all four sgRNA targets. This leads to a heterogeneous population of cells with mixed expression of at least one sgRNA target. Future CRISPRi designs should focus on multiple rounds of sgRNA lentiviral treatment in life-extended HFF-dCas9 cells to allow for greater opportunities to homogenize the cell population. As an alternative, the development of shRNA-mediated knockdown of SOAT1 gene expression could be used to test the importance of SOAT1 to HCMV replication. shRNA-mediated gene knockdown has previously been successful to show the role of SOAT1 in glioblastoma and prostate cancer<sup>102,106</sup>. Development of a SOAT1 gene knockdown model would provide stronger evidence into the importance of *de novo* CE biosynthesis to HCMV replication.



In addition to studying CE biosynthesis, we need to examine the breakdown of CE via hydrolysis. Enzymatic breakdown of CE into cholesterol and fatty acyl-CoA is mediated by cholesterol ester hydrolase (CEH) activity. Research has previously established that the related herpesvirus HSV-1 induces high CE accumulation, in part by reducing neutral CEH (NCEH) activity by 84%<sup>113</sup>. We can begin examining CE hydrolysis by measuring NCEH expression during HCMV replication. Given that there are significantly greater levels of CE in infected cells, we predict that HCMV suppresses CE hydrolysis while supporting CE biosynthesis.

HCMV requires host lipid metabolism to supply the building blocks and energy required to produce infectious viral progeny. We performed an untargeted lipidomic screen and found that HCMV-infected cells had elevated CE lipids by 24 hpi. Our overall hypothesis was that early stages of HCMV replication promote CE biosynthesis and that this pathway can be targeted to block viral replication. We characterized CE lipid biosynthesis by discovering HCMV increases SOAT1 gene expression early during viral replication. Further, HCMV strongly induced unsaturated VLCFA-CE lipids, which normally compose less than 0.3% of total CE lipids in uninfected HFF cells. We next examined potential viral mechanisms of inducing CE accumulation. We found that HCMV induces CE accumulation, in part, by immediate early pUL37x1. However, PERK suppresses CE accumulation during infection. Finally, we focused on SOAT1-mediated CE biosynthesis as a potential antiviral target. We discovered that avasimibe blocks HCMV replication by interfering with early protein expression. Further examining the effects of avasimibe on viral replication could provide new antiviral therapies against HCMV<sup>160</sup>.

## Chapter 5: References

1. Pellett, P. E. & Roizman, B. Herpesviridae. in *Fields Virology* (eds. Knipe, D. M. & Howley, P. M.) **2**, (Lippincott Williams & Wilkins, 2013).
2. Manicklal, S., Emery, V. C., Lazzarotto, T., Boppana, S. B. & Gupta, R. K. The 'Silent' Global Burden of Congenital Cytomegalovirus. *Clin. Microbiol. Rev.* **26**, 86–102 (2013).
3. Cannon, M. J., Schmid, D. S. & Hyde, T. B. Review of cytomegalovirus seroprevalence and demographic characteristics associated with infection. *Rev. Med. Virol.* **20**, 202–213 (2010).
4. Cannon, M. J. Congenital cytomegalovirus (CMV) epidemiology and awareness. *J. Clin. Virol.* 6–10 (2009). doi:10.1016/j.jcv.2009.09.002
5. Cannon, M. J., Hyde, T. B. & Schmid, D. S. Review of cytomegalovirus shedding in bodily fluids and relevance to congenital cytomegalovirus infection. *Rev. Med. Virol.* **21**, 240–255 (2015).
6. Joseph, S. A., Béliveau, C., Muecke, C. J. & Rahme, E. Cytomegalovirus as an occupational risk in daycare educators. *Pediatr. Child Heal.* **11**, 401–407 (2006).
7. Schleiss, M. R. Cytomegalovirus Vaccine Development. in *Human Cytomegalovirus*. (eds. Shenk, T. E. & Stinski, M. F.) 361–382 (Springer, 2008).
8. Dahle, A. J., Fowler, K. B., Wright, J. D. & Pass, R. F. Longitudinal Investigation of Hearing Disorders in Children with Congenital Cytomegalovirus. *J. Am. Acad. Audiol.* **11**, 283–290 (2000).
9. Fowler, K. B. & Boppana, S. B. Congenital cytomegalovirus (CMV) infection and hearing deficit. *J. Clin. Virol.* **35**, 226–231 (2006).
10. Britt, W. Manifestations of Human Cytomegalovirus Infection : Proposed Mechanisms of Acute and Chronic Disease. in *Human Cytomegalovirus*. (eds. Shenk, T. E. & Stinski, M. F.) 417–470 (Springer, 2008).
11. Britt, W. J. Congenital Human Cytomegalovirus Infection and the Enigma of Maternal Immunity. *J. Virol.* **91**, 1–7 (2017).
12. Huang, E.-S., Alford, C. A., Reynolds, D. W., Stagno, S. & Pass, R. F. Molecular Epidemiology of Cytomegalovirus Infections in Women and their Infants. *N. Engl. J. Med.* **303**, 958–962 (1980).
13. Ross, S. A. *et al.* Cytomegalovirus (CMV) Reinfections in Healthy Seroimmune Women. *J. Infect. Dis.* **201**, 386–389 (2011).
14. Boppana, S. B., Rivera, L. B., Fowler, K. B., Mach, M. & Britt, W. J. Intrauterine Transmission of Cytomegalovirus to Infants of Women with Preconceptional Immunity. *N. Engl. J. Med.* **344**, 1366–1371 (2001).

15. Yamamoto, A. Y. *et al.* Human cytomegalovirus reinfection is associated with intrauterine transmission in a highly cytomegalovirus-immune maternal population. *Am. J. Obstet. Gynecol.* **202**, (2010).
16. Kenneson, A. & Cannon, M. J. Review and meta-analysis of the epidemiology of congenital cytomegalovirus (CMV) infection. *Rev. Med. Virol.* **17**, 253–276 (2007).
17. Pereboom, M. T. R., Manniën, J., Spelten, E. R., Schellevis, F. G. & Hutton, E. K. Observational study to assess pregnant women's knowledge and behaviour to prevent toxoplasmosis, listeriosis and cytomegalovirus. *BMC Pregnancy Childbirth* **13**, (2013).
18. Grazia, M. *et al.* Prevention of Primary Cytomegalovirus Infection in Pregnancy. *EBioMedicine* **2**, 1205–1210 (2015).
19. Rowshani, A. T., Bemelman, F. J., van Leeuwen, E. M. M., van Lier, R. A. & ten Berge, I. J. M. Clinical and Immunologic Aspects of Cytomegalovirus Infection in Solid Organ Transplant Recipients. *Transplantation* **79**, 381–386 (2005).
20. Cainelli, F. & Vento, S. Infections and solid organ transplant rejection: a cause-and-effect relationship? *Lancet Infect. Dis.* **2**, 539–549 (2002).
21. Salzberger, B. B., Bowden, R. A., Hackman, R. C., Davis, C. & Boeckh, M. Neutropenia in Allogeneic Marrow Transplant Recipients Receiving Ganciclovir for Prevention of Cytomegalovirus Disease: Risk Factors and Outcome. *Blood* **90**, 2502–2508 (1997).
22. Britt, W. J. & Prichard, M. N. New therapies for human cytomegalovirus infections. *Antiviral Res.* **159**, 153–174 (2018).
23. Michaelis, M., Doerr, H. W. & Cinatl, J. The Story of Human Cytomegalovirus and Cancer: Increasing Evidence and Open Questions. *Neoplasia* **11**, 1–9 (2009).
24. Cobbs, C. S. *et al.* Human Cytomegalovirus Infection and Expression in Human Malignant Glioma. *Cancer Res.* **62**, 3347–3350 (2002).
25. Popović, M. *et al.* Human cytomegalovirus infection and atherothrombosis. *J. Thromb. Thrombolysis* **33**, 160–172 (2012).
26. Jan, C., Benedi, J., Ho, J. & Jeli, I. The possible role of human cytomegalovirus (HCMV) in the origin of atherosclerosis. *J. Clin. Virol.* **16**, 17–24 (2000).
27. Rahbar, A., Orrego, A., Peredo, I., Dzabic, M. & Wolmer-solberg, N. Human cytomegalovirus infection levels in glioblastoma multiforme are of prognostic value for survival. *J. Clin. Virol.* **57**, 36–42 (2013).
28. Israel, B. & Medical, D. Survival in Patients with Glioblastoma Receiving Valganciclovir. *N. Engl. J. Med.* **369**, 985–986 (2013).
29. Price, R. L. *et al.* Cytomegalovirus Contributes to Glioblastoma in the Context of Tumor Suppressor Mutations. *Tumor Stem Cell Biol.* **73**, 3441–3451 (2013).

30. Zhou, Y. F., Finkel, T. & Epstein, S. E. Human cytomegalovirus increases modified low density lipoprotein uptake and scavenger receptor mRNA expression in vascular smooth muscle cells. *J. Clin. Invest.* **98**, 2129–2138 (1996).
31. Gibson, W. Structure and Formation of the Cytomegalovirus Virion. in *Human Cytomegalovirus*. (eds. Shenk, T. E. & Stinski, M. F.) 187–204 (Springer, 2008).
32. Murphy, E. Human Cytomegalovirus Genome. in *Human Cytomegalovirus*. (eds. Shenk, T. E. & Stinski, M. F.) 1–19 (Springer, 2008).
33. Stern-ginossar, N. *et al.* Decoding Human Cytomegalovirus. *Sci. Reports* **338**, 1088–1094 (2012).
34. Oduro, J. D., Uecker, R., Hagemeyer, C. & Wiebusch, L. Inhibition of Human Cytomegalovirus Immediate-Early Gene Expression by Cyclin A2-Dependent Kinase Activity. *J. Virol.* **86**, 9369–9383 (2012).
35. Parit, G. S. & Anders, D. G. Eleven Loci Encoding trans-Acting Factors Are Required for Transient Complementation of Human Cytomegalovirus oriLyt-Dependent DNA Replication. *J. Virol.* **67**, 6979–6988 (1993).
36. Leach, F. S. & Mocarski, E. S. Regulation of Cytomegalovirus Late-Gene Expression : Differential Use of Three Start Sites in the Transcriptional Activation of ICP36 Gene Expression. *J. Virol.* **63**, 1783–1791 (1989).
37. Huang, E.-S. Specific Inhibition of Virus-Induced DNA Polymerase Activity and Viral DNA REplication by Phosphonoacetic Acid. *J. Virol.* **16**, 1560–1565 (1975).
38. Digel, M. & Jahn, G. Cytomegalovirus Cell Tropism. in *Human Cytomegalovirus*. (eds. Shenk, T. E. & Stinski, M. F.) 63–83 (Springer, 2008).
39. Cheng, S., Caviness, K., Buehler, J., Smithey, M. & Ž, J. N.-. Transcriptome-wide characterization of human cytomegalovirus in natural infection and experimental latency. *PNAS* **11**, (2017).
40. Leng, S. X. *et al.* Recent advances in CMV tropism, latency, and diagnosis during aging. *GeroScience* **39**, 251–259 (2017).
41. Reeves, M. & Sinclair, J. Aspects of Human Cytomegalovirus Latency and Reactivation. in *Human Cytomegalovirus*. (eds. Shenk, T. E. & Stinski, M. F.) 297–313 (Springer, 2008).
42. Goodrum, F., Caviness, K. & Zagallo, P. Human Cytomegalovirus Persistence. *Cell Microbiol.* **14**, 644–655 (2012).
43. Collins-McMillen, D., Buehler, J., Peppenelli, M. & Goodrum, F. Molecular Determinants and the Regulation of Human Cytomegalovirus Latency and Reactivation. *Viruses* **10**, 1–27 (2018).
44. Kim, J. H., Collins-McMillen, D., Buehler, J. C., Goodrum, F. D. & Yurochko, A. D. Human Cytomegalovirus Requires Epidermal Growth Factor Receptor Signaling to Enter and Initiate the Early Steps in the Establishment of Latency in CD34+

- Human Progenitor Cells. *J. Virol.* **91**, 1–21 (2017).
45. Zhu, D. *et al.* Human cytomegalovirus reprogrammes haematopoietic progenitor cells into immunosuppressive monocytes to achieve latency. *Nat. Microbiol.* **3**, 503–513 (2018).
  46. Goodrum, F. D., Jordan, C. T., High, K. & Shenk, T. Human cytomegalovirus gene expression during infection of primary hematopoietic progenitor cells : A model for latency. *PNAS* **99**, 16255–16260 (2002).
  47. McArdle, J., Moorman, N. J. & Munger, J. HCMV targets the metabolic stress response through activation of AMPK whose activity is important for viral replication. *PLoS Pathog.* **8**, 1–10 (2012).
  48. Yu, Y., Maguire, T. G. & Alwine, J. C. Human Cytomegalovirus Activates Glucose Transporter 4 Expression To Increase Glucose Uptake during Infection. *J. Virol.* **85**, 1573–1580 (2011).
  49. Munger, J. *et al.* Systems-level metabolic flux profiling identifies fatty acid synthesis as a target for antiviral therapy. *Nat. Biotechnol.* **26**, 1179–1186 (2008).
  50. Munger, J., Bajad, S. U., Collier, H. A., Shenk, T. & Rabinowitz, J. D. Dynamics of the cellular metabolome during human cytomegalovirus infection. *PLoS Pathog.* **2**, 1165–1175 (2006).
  51. Xu, H. *et al.* Acyl-CoA synthetase short-chain family member 2 (ACSS2) is regulated by SREBP-1 and plays a role in fatty acid synthesis in caprine mammary epithelial cells. *J. Cell. Physiol.* **233**, 1005–1016 (2018).
  52. Spencer, C. M., Schafer, X. L., Moorman, N. J. & Munger, J. Human Cytomegalovirus Induces the Activity and Expression of Acetyl-Coenzyme A Carboxylase, a Fatty Acid Biosynthetic Enzyme Whose Inhibition Attenuates Viral Replication. *J. Virol.* **85**, 5814–5824 (2011).
  53. Koyuncu, E., Purdy, J. G., Rabinowitz, J. D. & Shenk, T. Saturated Very Long Chain Fatty Acids Are Required for the Production of Infectious Human Cytomegalovirus Progeny. *PLoS Pathog.* **9**, 1–15 (2013).
  54. Purdy, J. G., Shenk, T. & Rabinowitz, J. D. Fatty acid elongase 7 catalyzes lipidome remodeling essential for human cytomegalovirus replication. *Cell Rep.* **10**, 1375–1385 (2015).
  55. Yu, Y., Maguire, T. G. & Alwine, J. C. Human Cytomegalovirus Infection Induces Adipocyte-Like Lipogenesis through Activation of Sterol Regulatory Element Binding Protein 1. *J. Virol.* **86**, 2942–2949 (2012).
  56. Yu, Y., Maguire, T. G. & Alwine, J. C. ChREBP, a glucose-responsive transcriptional factor, enhances glucose metabolism to support biosynthesis in human cytomegalovirus-infected cells. *PNAS* **111**, 1951–1956 (2014).
  57. Regan, N. G., Greco, T. M., Cristea, I. M. & Shenk, T. Increased Expression of

- LDL Receptor-Related Protein 1 during Human Cytomegalovirus Infection Reduces Virion Cholesterol and Infectivity. *Cell Host Microbe* **12**, 86–96 (2012).
58. Debose-boyd, R. A. & Ye, J. SREBPs in Lipid Metabolism, Insulin Signaling, and Beyond. *Trends Biochem. Sci.* **43**, 358–368 (2018).
  59. Postic, C., Dentin, R., Denechaud, P. & Girard, J. ChREBP, a Transcriptional Regulator of Glucose and Lipid Metabolism. *Annu. Rev. Nutr.* **27**, 179–192 (2007).
  60. Isler, J. A., Skalet, A. H. & Alwine, J. C. Human Cytomegalovirus Infection Activates and Regulates the Unfolded Protein Response. *J. Virol.* **79**, 6890–6899 (2005).
  61. Yu, Y., Jr, F. J. P., Maguire, T. G. & Alwine, J. C. PKR-Like Endoplasmic Reticulum Kinase Is Necessary for Lipogenic Activation during HCMV Infection. *PLoS Pathog.* **9**, (2013).
  62. Cavener, D. R., Gupta, S. & Mcgrath, B. C. PERK in beta cell biology and insulin biogenesis. *Trends Endocrinol. Metab.* **21**, (2010).
  63. Bobrovnikova-Marjon, E. *et al.* PERK Utilizes Intrinsic Lipid Kinase Activity To Generate Phosphatidic Acid, Mediate Akt Activation, and Promote Adipocyte Differentiation. *Mol. Cell. Biol.* **32**, 2268–2278 (2012).
  64. Moorman, N. J. *et al.* Human Cytomegalovirus Protein UL38 Inhibits Host Cell Stress Responses by Antagonizing the Tuberous Sclerosis Protein Complex. *Cell Host Microbe* 253–262 (2008). doi:10.1016/j.chom.2008.03.002
  65. Rauwel, B. *et al.* Activation of Peroxisome Proliferator-Activated Receptor Gamma by Human Cytomegalovirus for De Novo Replication Impairs Migration and Invasiveness of Cytotrophoblasts from Early Placentas □. *J. Virol.* **84**, 2946–2954 (2010).
  66. Lehrke, M. & Lazar, M. A. The Many Faces of PPAR $\gamma$ . *Cell* **123**, 993–999 (2005).
  67. Rolland, M. *et al.* PPAR $\gamma$  Is Activated during Congenital Cytomegalovirus Infection and Inhibits Neuronogenesis from Human Neural Stem Cells. *PLOS Pathog.* **12**, 1–30 (2016).
  68. Cho, H. J., Park, J., Lee, H. W., Lee, Y. S. & Kim, J. B. Regulation of adipocyte differentiation and insulin action with rapamycin. *Biomed. Biophys. Res. Commun.* **321**, 942–948 (2004).
  69. Kim, J. E. & Chen, J. Regulation of Peroxisome Proliferator-Activated Receptor- $\gamma$  Activity by Mammalian Target of Rapamycin and Amino Acids in Adipogenesis. *Diabetes* **53**, (2004).
  70. Storck, E. M., Özbalci, C. & Eggert, U. S. Lipid Cell Biology: A Focus on Lipids in Cell Division. *Annu. Rev. Biochem.* **87**, 839–869 (2018).
  71. Fahy, E. *et al.* A comprehensive classification system for lipids. *J. Lipid Res.* **46**,

- 839–862 (2005).
72. Thiam, A. R., Farese, R. V. & Walther, T. C. The biophysics and cell biology of lipid droplets. *Nat. Rev. Mol. Cell Biol.* **14**, 775–786 (2013).
  73. Goedeke, L. & Fernández-Hernando, C. Regulation of cholesterol homeostasis. *Cell. Mol. Life Sci.* **69**, 915–930 (2012).
  74. Tabas, I. Consequences of cellular cholesterol accumulation : Basic concepts and physiological implications. *J. Clin. Invest.* **110**, 905–911 (2002).
  75. Warner, G. J., Stoudt, G., Bamberger, M., Johnson, W. J. & Rothblat, G. H. Cell Toxicity Induced by Inhibition of Acyl Coenzyme A:Cholesterol Acyltransferase and Accumulation of Unesterified Cholesterol. *J. Biol. Chem.* **270**, 5772–5778 (1995).
  76. Green, P. H. R. & Glickman, R. M. Intestinal lipoprotein metabolism. *J. Lipid Res.* **22**, 1153–73 (1981).
  77. Schneider, W. J. Lipoprotein Receptors. in *Biochemistry of Lipids, Lipoproteins and Membranes*. (eds. Rdigway, N. D. & McLeod, R. S.) 489–518 (Elsevier, 2016). doi:10.1016/B978-0-444-63438-2.00017-1
  78. Anderson, R. G. W., Brown, M. S. & Goldstein, J. L. Role of the coated endocytic vesicle in the uptake of receptor-bound low density lipoprotein in human fibroblasts. *Cell* **10**, 351–364 (1977).
  79. Goldstein, J. L. & Brown, M. S. A century of cholesterol and coronaries: From plaques to genes to statins. *Cell* **161**, 161–172 (2015).
  80. Jonas, A. Lecithin cholesterol acyltransferase. *Biochim. Biophys. Acta* **1529**, 245–256 (2000).
  81. Rogers, M. A. *et al.* Acyl-CoA:cholesterol acyltransferases (ACATs/SOATs): Enzymes with multiple sterols as substrates and as activators. *J. Steroid Biochem. Mol. Biol.* **151**, 102–107 (2015).
  82. Lin, S., Cheng, D., Liu, M. S., Chen, J. & Chang, T. Y. Human acyl-CoA:cholesterol acyltransferase-1 in the endoplasmic reticulum contains seven transmembrane domains. *J. Biol. Chem.* **274**, 23276–23285 (1999).
  83. Chang, T., Li, B., Chang, C. C. Y. & Urano, Y. Acyl-coenzyme A: cholesterol acyltransferases. *Am. J. Physiol. Endocrinol. Metab.* **297**, 1–9 (2009).
  84. Chang, C. C. Y. *et al.* Immunological quantitation and localization of ACAT-1 and ACAT-2 in human liver and small intestine. *J. Biol. Chem.* **275**, 28083–28092 (2000).
  85. Li, B. L. *et al.* Human acyl-CoA:cholesterol acyltransferase-1 (ACAT-1) gene organization and evidence that the 4.3-kilobase ACAT-1 mRNA is produced from two different chromosomes. *J. Biol. Chem.* **274**, 11060–11071 (1999).

86. Yang, L. *et al.* Human acyl-coenzyme A:cholesterol acyltransferase 1 (acat1) sequences located in two different chromosomes (7 and 1) are required to produce a novel ACAT1 isoenzyme with additional sequence at the N terminus. *J. Biol. Chem.* **279**, 46253–46262 (2004).
87. Cases, S. *et al.* ACAT-2 , A Second Mammalian Acyl-CoA : Cholesterol Acyltransferase. *J. Biol. Chem.* **273**, 26755–26764 (1998).
88. Song, B.-L. *et al.* Human acyl-CoA:cholesterol acyltransferase 2 gene expression in intestinal Caco-2 cells and in hepatocellular carcinoma. *Biochem. J.* **394**, 617–626 (2006).
89. Chang, C. C. Y. *et al.* Recombinant acyl-coA:cholesterol acyltransferase-1 (ACAT-1) purified to essential homogeneity utilizes cholesterol in mixed micelles or in vesicles in a highly cooperative manner. *J. Biol. Chem.* **273**, 35132–35141 (1998).
90. Rogers, M. A. *et al.* Cellular pregnenolone esterification by Acyl-CoA:cholesterol acyltransferase. *J. Biol. Chem.* **287**, 17483–17492 (2012).
91. Shibuya, Y. & Chang, C. C. Y. ACAT1/SOAT1 as a therapeutic target for Alzheimer's disease. *Future Med. Chem.* **7**, 2451–2467 (2015).
92. Huff, M. W., Daugherty, A. & Lu, H. Atherosclerosis. in *Biochemistry of Lipids, Lipoproteins and Membranes* (eds. Ridgway, N. D. & McLeod, R. S.) 519–548 (Elsevier, 2016). doi:10.1016/B978-0-444-63438-2.00018-3
93. Yang, L. *et al.* Enhancement of human ACAT1 gene expression to promote the macrophage-derived foam cell formation by dexamethasone. *Cell Res.* **14**, 315–323 (2004).
94. Accad, M. *et al.* Massive xanthomatosis and altered composition of atherosclerotic lesions in hyperlipidemic mice lacking acyl CoA : cholesterol acyltransferase 1. *J. Clin. Invest.* **105**, 711–719 (2000).
95. Yagyu, H. *et al.* Absence of ACAT-1 Attenuates Atherosclerosis but Causes Dry Eye and Cutaneous Xanthomatosis in Mice with Congenital Hyperlipidemia. *J. Biol. Chem.* **275**, 21324–21330 (2000).
96. Lunardi, C. *et al.* Endothelial Cells ' Activation and Apoptosis Induced by a Subset of Antibodies against Human Cytomegalovirus : Relevance to the Pathogenesis of Atherosclerosis. *PLoS One* (2007). doi:10.1371/journal.pone.0000473
97. Wu, T. *et al.* Demonstration of Cytomegalovirus Nucleic Acids in the Coronary Arteries of Transplanted Hearts. *Am. J. Pathol.* **140**, 739–747 (1992).
98. Hendrix, M. G. R. & Daemen, M. Cytomegalovirus Nucleic Acid Distribution Within the Human Vascular Tree. *Am. J. Pathol.* **138**, 563–567 (1991).
99. Beloribi-djefa, S., Vasseur, S. & Guillaumond, F. Lipid metabolic reprogramming in cancer cells. *Oncogenesis* **5**, (2016).



100. Santos, C. R. & Schulze, A. Lipid metabolism in cancer. *FEBS Minireview* **279**, 2610–2623 (2012).
101. Gaglio, D. *et al.* Oncogenic K-Ras decouples glucose and glutamine metabolism to support cancer cell growth. *Mol. Syst. Biol.* **7**, 1–15 (2011).
102. Geng, F. *et al.* Inhibition of SOAT1 Suppresses Glioblastoma Growth via Blocking SREBP-1 – Mediated Lipogenesis. *Clin. Cancer Res.* **22**, 5337–5348 (2016).
103. Antalis, C. J., Arnold, T., Lee, B., Buhman, K. K. & Siddiqui, R. A. Docosahexaenoic acid is a substrate for ACAT1 and inhibits cholesteryl ester formation from oleic acid in MCF-10A cells. *Prostaglandins Leukot. Essent. Fat. Acids* **80**, 165–171 (2009).
104. Abramczyk, H., Surmacki, J., Olejnik, A. K., Lubecka-pietruszewska, K. & Fabianowska-majewska, K. The role of lipid droplets and adipocytes in cancer. Raman imaging of cell cultures: MCF10A, MCF7, and MDA-MB-231 compared to adipocytes in cancerous human breast tissue. *Analyst* **140**, 2224–2235 (2015).
105. Accioly, M. T. *et al.* Lipid Bodies Are Reservoirs of Cyclooxygenase-2 and Sites of Prostaglandin-E 2 Synthesis in Colon Cancer Cells. *Cancer Res.* **68**, 1732–1741 (2008).
106. Yue, S. *et al.* Cholesteryl Ester Accumulation Induced by PTEN Loss and PI3K/AK Activation Underlies Human Prostate Cancer Aggressiveness. *Cell Metab.* **19**, 393–406 (2015).
107. Li, J. *et al.* Abrogating cholesterol esterification suppresses growth and metastasis of pancreatic cancer. *Oncogene* **35**, 6378–6388 (2016).
108. Mitchell, D. A. *et al.* Sensitive detection of human cytomegalovirus in tumors and peripheral blood of patients diagnosed with glioblastoma. *Neuro. Oncol.* **10**, 10–18 (2007).
109. Samanta, M., Harkins, L., Klemm, K., Britt, W. J. & Cobbs, C. S. High Prevalence of Human Cytomegalovirus in Prostatic Intraepithelial Neoplasia and Prostatic Carcinoma. *J. Urol.* **170**, 998–1002 (2003).
110. Harkins, L. *et al.* Specific localisation of human cytomegalovirus nucleic acids and proteins in human colorectal cancer. *Lancet* **360**, 1557–1563 (2002).
111. Fabricant, C. G., Hajjar, D. P., Minick, C. R. & Fabricant, J. Herpesvirus Infection Enhances Cholesterol and Cholesteryl Ester Accumulation in Cultured Arterial Smooth Muscle Cells. *Am. J. Pathol.* **105**, 176–184 (1981).
112. Hajjar, D. P., Falcones, D. J. & Fabricant, C. G. Altered Cholesteryl Ester Cycle Is Associated with Lipid Accumulation in Herpesvirus-infected Arterial Smooth Muscle Cells \*. *J. Biol. Chem.* **260**, 6124–6128 (1985).
113. Hajjar, D. P., Weksler, B. B. & Grant, A. J. Herpes simplex virus infection in human arterial cells. Implications in arteriosclerosis. *J. Clin. Invest.* **80**, 1317–

- 1321 (1987).
114. Low, H. *et al.* Cytomegalovirus Restructures Lipid Rafts via a US28/CDC42-Mediated Pathway, Enhancing Cholesterol Efflux from Host Cells. *Cell Rep.* **16**, 186–200 (2016).
  115. Read, S. A., Tay, E., Shahidi, M., George, J. & Douglas, M. W. Hepatitis C virus infection mediates cholesteryl ester synthesis to facilitate infectious particle production. *J. Gen. Virol.* **95**, 1900–1910 (2014).
  116. Hu, L. *et al.* Avasimibe: A novel hepatitis C virus inhibitor that targets the assembly of infectious viral particles. *Antiviral Res.* **148**, 5–14 (2017).
  117. Merz, A. *et al.* Biochemical and Morphological Properties of Hepatitis C Virus Particles and Determination of Their Lipidome. *J. Biol. Chem.* **286**, 3018–3032 (2011).
  118. Loizides-Mangold, U. *et al.* HCV 3a Core Protein Increases Lipid Droplet Cholesteryl Ester Content via a Mechanism Dependent on Sphingolipid Biosynthesis. *PLoS One* **9**, 1–24 (2014).
  119. Chen, S. L. & Morgan, T. R. The Natural History of Hepatitis C Virus (HCV) Infection. *Int. J. Med. Sci.* **3**, 47–52 (2006).
  120. Machado, M. V, Oliveira, A. G. & Cortez-pinto, H. Hepatic steatosis in hepatitis B virus infected patients : Meta-analysis of risk factors and comparison with hepatitis C infected patients. *Gastroenterol. Hepatol.* **26**, 1361–1367 (2011).
  121. Agnello, V., Elfahal, M., Knight, G. B. & Zhang, Q. Hepatitis C virus and other Flaviviridae viruses enter cells via low density lipoprotein receptor. *PNAS* **96**, 12766–12771 (1999).
  122. Scarselli, E. *et al.* The human scavenger receptor class B type I is a novel candidate receptor for the hepatitis C virus. *EMBO* **21**, 5017–5025 (2002).
  123. Suzuki, T. Assembly of hepatitis C virus particles. *Microbiol. Immunol.* **55**, 12–18 (2011).
  124. Boyer, A. *et al.* The Association of Hepatitis C Virus Glycoproteins with Apolipoproteins E and B Early in Assembly Is Conserved in Lipoviral Particles \*. *J. Biol. Chem.* **289**, 18904–18913 (2014).
  125. Yu, D., Smith, G. A., Enquist, L. W. & Shenk, T. Construction of a Self-Excisable Bacterial Artificial Chromosome Containing the Human Cytomegalovirus Genome and Mutagenesis of the Diploid TRL/IRL13 Gene. *J. Virol.* **76**, 2316–2328 (2002).
  126. Wang, D., Bresnahan, W. & Shenk, T. Human cytomegalovirus encodes a highly specific RANTES decoy receptor. *Proc. Natl. Acad. Sci.* **101**, 16642–16647 (2004).
  127. Sharon-Friling, R., Goodhouse, J., Colberg-Poley, A. M. & Shenk, T. Human cytomegalovirus pUL37x1 induces the release of endoplasmic reticulum calcium

- stores. *PNAS* **103**, 19117–19122 (2006).
128. Vastag, L., Koyuncu, E., Grady, S. L., Shenk, T. E. & Rabinowitz, J. D. Divergent effects of human cytomegalovirus and herpes simplex virus-1 on cellular metabolism. *PLoS Pathog.* **7**, (2011).
  129. Kudchodkar, S. B., Yu, Y., Maguire, T. G. & Alwine, J. C. Human Cytomegalovirus Infection Induces Rapamycin-Insensitive Phosphorylation of Downstream Effectors of mTOR Kinase. *J. Virol.* **78**, 11030–11039 (2004).
  130. McArdle, J., Schafer, X. L. & Munger, J. Inhibition of Calmodulin-Dependent Kinase Kinase Blocks Human Cytomegalovirus-Induced Glycolytic Activation and Severely Attenuates Production of Viral Progeny. *J. Virol.* **85**, 705–714 (2011).
  131. Clippinger, A. J. & Alwine, J. C. Dynein mediates the localization and activation of mTOR in normal and human cytomegalovirus-infected cells. *Genes Dev.* **26**, 2015–2026 (2012).
  132. Clasquin, M. F., Melamud, E. & Rabinowitz, J. D. LC-MS Data Processing with MAVEN: A Metabolomic Analysis and Visualization Engine. *Curr. Protoc. Bioinforma.* **0**, 1–31 (2012).
  133. Melamud, E., Vastag, L. & Rabinowitz, J. D. Metabolomic analysis and visualization engine for LC-MS data. *Anal. Chem.* **82**, 9818–9826 (2010).
  134. Murphy, R. C. Steroids. in *Tandem Mass Spectrometry of Lipids: Molecular Analysis of Complex Lipids* (eds. Gaskell, S. J., Heeren, R. M. A. & Setou, M.) 233–273 (Royal Society of Chemistry, 2015).
  135. Munger, J., Yu, D. & Shenk, T. UL26-Deficient Human Cytomegalovirus Produces Virions with Hypophosphorylated pp28 Tegument Protein That Is Unstable within Newly Infected Cells. *J. Virol.* **80**, 3541–3548 (2006).
  136. Kalejta, R. F., Bechtel, J. T. & Shenk, T. Human Cytomegalovirus pp71 Stimulates Cell Cycle Progression by Inducing the Proteasome-Dependent Degradation of the Retinoblastoma Family of Tumor Suppressors. *Mol. Cell. Biol.* **23**, 1885–1895 (2003).
  137. Silva, M. C., Yu, Q., Enquist, L. & Shenk, T. Human Cytomegalovirus UL99-Encoded pp28 Is Required for the Cytoplasmic Envelopment of Tegument-Associated Capsids. *J. Virol.* **77**, 10594–10605 (2003).
  138. Zhu, H. U. A., Shen, Y. & Shenk, T. Human Cytomegalovirus IE1 and IE2 Proteins Block Apoptosis. *J. Virol.* **69**, 7960–7970 (1995).
  139. Sanjana, N. E., Shalem, O. & Zhang, F. Improved vectors and genome-wide libraries for CRISPR screening. *Nat. Publ. Gr.* **11**, 783–784 (2014).
  140. Kearns, N. A. *et al.* Cas9 effector-mediated regulation of transcription and differentiation in human pluripotent stem cells. *Development* **141**, 219–223 (2014).

141. Pham, H., Kearns, N. A. & Maehr, R. Transcriptional Regulation with CRISPR/Cas9 Effectors in Mammalian Cells. in *Post-Transcriptional Gene Regulation* (ed. Dassi, E.) **1358**, 43–57 (Humana Press, 2016).
142. Du, K. *et al.* Activation of a Metabolic Gene Regulatory Network Downstream of mTOR Complex 1. *Cell Mol. Cell* **39**, 171–183 (2010).
143. Bugge, A., Grøntved, L., Aagaard, M. M., Borup, R. & Mandrup, S. The PPAR $\gamma$ 2 A/B-Domain Plays a Gene-Specific Role in Transactivation and Cofactor Recruitment. *Mol. Endocrinol.* **23**, 794–808 (2009).
144. Shenk, T. & Alwine, J. C. Human Cytomegalovirus: Coordinating Cellular Stress, Signaling, and Metabolic Pathways. *Annu. Rev. Virol.* **1**, 355–374 (2014).
145. Cells, E. *et al.* Hydroxymethyl-Glutaryl Coenzyme A Reductase Inhibition Limits Cytomegalovirus Infection in Human Endothelial Cells. *Circulation* **109**, 532–536 (2004).
146. Averous, J. *et al.* The eIF2 $\alpha$ /ATF4 pathway is essential for stress-induced autophagy gene expression. *Nucleic Acids Res.* **41**, 7683–7699 (2013).
147. Singh, R. *et al.* Autophagy regulates lipid metabolism. *Nature* **458**, 1131–1135 (2009).
148. Chaumorcel, M., Souquère, S., Pierron, G., Codogno, P. & Esclatine, A. Human cytomegalovirus controls a new autophagy-dependent cellular antiviral defense mechanism. *Autophagy* **41**, 46–53 (2008).
149. Chaumorcel, M. *et al.* The Human Cytomegalovirus Protein TRS1 Inhibits Autophagy via Its Interaction with Beclin 1. *J. Virol.* **86**, 2571–2584 (2012).
150. Llaverías, G., Laguna, J. C. & Alegret, M. Pharmacology of the ACAT inhibitor avasimibe (CI-1011). *Cardiovasc. Drug Rev.* **21**, 33–50 (2003).
151. Sugiyama, Y. *et al.* TMP-153 , a novel ACAT inhibitor, lowers plasma cholesterol through its hepatic action in Golden hamsters. *Atherosclerosis* **118**, 145–153 (1995).
152. Sugi, Y. *et al.* TMP-153 , a novel ACAT inhibitor , inhibits cholesterol absorption and lowers plasma cholesterol in rats and hamsters. *Atherosclerosis* **13**, 71–78 (1995).
153. Lee, H. T. *et al.* Inhibitors of Acyl-CoA:cholesterol O-Acyl transferase (ACAT) as hypocholesterolemic agents. CI-1011: An acyl sulfamate with unique cholesterol-lowering activity in animals fed noncholesterol-supplemented diets. *J. Med. Chem.* **39**, 5031–5034 (1996).
154. Mandegar, M. A. *et al.* CRISPR Interference Efficiently Induces Specific and Reversible Gene Silencing in Human iPSCs. *Cell Stem Cell* **18**, 541–553 (2017).
155. Mcleod, R. S. & Yao, Z. Assembly and Secretion of Triglyceride-Rich Lipoproteins. in *Biochemistry of Lipids, Lipoproteins and Membranes*. 459–488

- (Elsevier, 2016). doi:10.1016/B978-0-444-63438-2.00016-X
156. Bozidis, P., Williamson, C. D. & Colberg-Poley, A. M. Mitochondrial and Secretory Human Cytomegalovirus UL37 Proteins Traffic into Mitochondrion-Associated Membranes of Human Cells. *J. Virol.* **82**, 2715–2726 (2008).
  157. Qian, Z., Xuan, B., Chapa, T. J., Gualberto, N. & Yu, D. Murine Cytomegalovirus Targets Transcription Factor ATF4 To Exploit the Unfolded-Protein Response. *J. Virol.* **86**, 6712–6723 (2012).
  158. McFarlane, S. *et al.* Early Induction of Autophagy in Human Fibroblasts after Infection with Human Cytomegalovirus or Herpes Simplex Virus 1 □. *J. Virol.* **85**, 4212–4221 (2011).
  159. Mukhopadhyay, R., Venkatadri, R., Katsnelson, J. & Arav-Boger, R. Digitoxin Suppresses Human Cytomegalovirus Replication via Na<sup>+</sup>, K<sup>+</sup>/ATPase α1 Subunit-Dependent AMP-Activated Protein Kinase and Autophagy Activation. *J. Virol.* **92**, 1–16 (2018).
  160. Insull, W. *et al.* Efficacy and short-term safety of a new ACAT inhibitor, avasimibe, on lipids, lipoproteins, and apolipoproteins, in patients with combined hyperlipidemia. *Atherosclerosis* **157**, 137–144 (2001).
  161. Wendel, A. A., Lewin, T. M. & Coleman, R. A. Glycerol-3-phosphate acyltransferases: Rate limiting enzymes of triacylglycerol biosynthesis. *Biochim. Biophys. Acta* **1791**, 501–506 (2009).
  162. Kuscu, C., Arslan, S., Singh, R., Thorpe, J. & Adli, M. Genome-wide analysis reveals characteristics of off-target sites bound by the Cas9 endonuclease. *Nat. Biotechnol.* **32**, 1–9 (2014).
  163. Mikkelsen, T. S. *et al.* Genome-wide maps of chromatin state in pluripotent and lineage-committed cells. *Nature* **448**, 553–562 (2007).
  164. Qi, L. S. *et al.* Repurposing CRISPR as an RNA-Guided Platform for Sequence-Specific Control of Gene Expression. *Cell Resour.* **8**, 1173–1183 (2013).